

**A NON-BIOMIMETIC APPROACH  
FOR PRODUCING SHANK KINEMATICS AND ENERGETICS  
DURING THE STANCE PHASE OF GAIT**

by

Travis Pollen

A thesis submitted to the Faculty of the University of Delaware in partial fulfillment of the requirements for the degree of Master of Science in Biomechanics and Movement Science

Summer 2015

© 2015 Travis Pollen  
All Rights Reserved

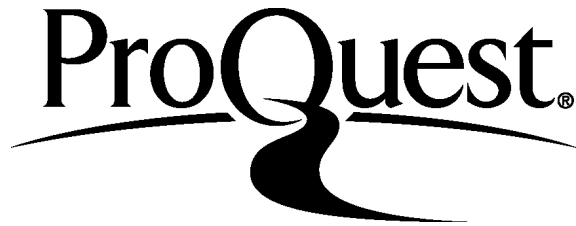
ProQuest Number: 1602370

All rights reserved

INFORMATION TO ALL USERS

The quality of this reproduction is dependent upon the quality of the copy submitted.

In the unlikely event that the author did not send a complete manuscript and there are missing pages, these will be noted. Also, if material had to be removed, a note will indicate the deletion.



ProQuest 1602370

Published by ProQuest LLC (2015). Copyright of the Dissertation is held by the Author.

All rights reserved.

This work is protected against unauthorized copying under Title 17, United States Code  
Microform Edition © ProQuest LLC.

ProQuest LLC.  
789 East Eisenhower Parkway  
P.O. Box 1346  
Ann Arbor, MI 48106 - 1346

**A NON-BIOMIMETIC APPROACH  
FOR PRODUCING SHANK KINEMATICS AND ENERGETICS  
DURING THE STANCE PHASE OF GAIT**

by

Travis Pollen

Approved: \_\_\_\_\_  
Steven J. Stanhope, Ph.D.  
Professor in charge of thesis on behalf of the Advisory Committee

Approved: \_\_\_\_\_  
C. Buz Swanik, Ph.D.  
Director of the Biomechanics and Movement Science Program

Approved: \_\_\_\_\_  
Kathleen S. Matt, Ph.D.  
Dean of the College of Health Science

Approved: \_\_\_\_\_  
James G. Richards, Ph.D.  
Vice Provost for Graduate and Professional Education

## **ACKNOWLEDGMENTS**

First, I would like to thank the University of Delaware Office of Graduate and Professional Education for funding this research through the University Graduate Scholar Award. I would also like to thank my advisor, Dr. Steven Stanhope, for constantly challenging me and pushing me beyond what I thought I was capable of. Additional thanks go to the other members of my committee, Dr. Elisa Arch, Dr. Todd Royer, and Dr. Thomas Kaminski, for their insights and tough questions, as well as Dr. Jeremy Crenshaw and Dr. Ryan Pohlig, for their help with the statistical aspects of the project.

This work would not have been possible were it not for the abundant help I received from my lab mates, both past and present: Dr. Kota Takahashi, Alexander Razzook, Lakisha Guinn, Anahid Ebrahimi, and John-David Collins. I thank them for always be willing to brainstorm, proofread, and chat. Finally, many thanks to my girlfriend, Kate Maum, for be so understanding as deadlines loomed, and my parents, for bearing me with a missing leg so I could identify firsthand with the amputee plight.

## TABLE OF CONTENTS

LIST OF TABLES .....	vi
LIST OF FIGURES .....	vii
ABSTRACT .....	xi
Chapter	
1 INTRODUCTION AND SPECIFIC AIMS .....	1
2 RESEARCH STRATEGY .....	12
2.1 Significance .....	12
2.2 Innovation.....	12
2.3 Approach .....	13
2.3.1 Participants .....	13
2.3.2 Data Collection .....	14
2.3.3 Data Processing, Definitions, and Analysis .....	15
2.3.4 Kinematics of Shank Progression.....	17
2.3.4.1 Kinematic Model .....	17
2.3.4.2 Point of Rotation.....	18
2.3.5 Energetics of Shank Progression .....	19
2.3.5.1 Validation of Net Segmental Power .....	20
2.3.6 Telescoping Inverted Pendulum Shank Model.....	21
2.3.6.1 Telescoping Shank Powers.....	21
2.3.7 Statistical Analysis .....	22
3 RESULTS.....	23
3.1 Kinematics of Shank Progression.....	23
3.1.1 Shank Angle .....	24
3.1.2 Shank Translation .....	26

3.1.3	Pivot Point Approximation.....	27
3.2	Energetics of Shank Progression.....	29
3.2.1	Validation of Shank Net Segmental Power.....	29
3.2.2	Shank Segmental Power at Push-off.....	30
3.3	Telescoping Inverted Pendulum Shank Model.....	31
3.3.1	Telescoping Knee Joint Center Position.....	34
3.3.2	Telescoping Shank Powers.....	34
4	DISCUSSION.....	37
4.1	Kinematics of Shank Progression.....	37
4.2	Energetics of Shank Progression.....	40
4.3	Telescoping Inverted Pendulum Shank Model.....	40
4.4	Delimitations and Future Directions.....	41
	REFERENCES.....	43
Appendices		
A	SUPPLEMENTAL DATA.....	48
B	INFORMED CONSENT.....	57
C	HUMAN SUBJECTS PROTOCOL.....	63

## LIST OF TABLES

Table 1	Participant characteristics.....	13
Table 2	Definition of stance-phase gait event placement.....	16
Table 3	Angular excursions by rocker, means and standard deviations.....	25
Table 4	Mean relative contributions across all participants of ankle and foot-to-floor angles to shank angle during stance at walking velocity 0.8 BH/s.....	26
Table 5	Mean perpendicular distance of approximation for the pivot point (PDA) .....	28
Table 6	Mean segmental power terms for all participants at peak ankle power ..	31
Table 7	Maximum telescoping distance .....	33
Table 8	Ankle angle excursions, by rocker .....	48
Table 9	Foot-to-floor angle excursions, by rocker .....	48
Table 10	Shank angle excursions, by rocker .....	49
Table 11	Bland-Altman mean differences averaged across participants, by gait event .....	49
Table 12	Bland-Altman mean lower limits of agreement averaged across participants, by gait event.....	50
Table 13	Bland-Altman mean upper limits of agreement averaged across participants, by gait event.....	50
Table 14	Intraclass correlation (3,2), by gait event .....	51

## LIST OF FIGURES

Figure 1	The stance phase of gait can be subdivided into four rockers, denoted by the anatomical landmarks about which the foot and shank pivot.....	1
Figure 2	The kinematics (rotations and translations) of the foot and shank arise from the interplay between the foot-to-floor and ankle angles. Figure adapted from <a href="http://www.istockphoto.com/photo/foot-bones-side-view-18523806">http://www.istockphoto.com/photo/foot-bones-side-view-18523806</a> .....	3
Figure 3	The energetics of a segment can be described by the flow of power into and out of its distal and proximal ends via muscle moment powers (red) and joint force powers (blue). ....	4
Figure 4	Roll-over shape (red arc) denotes the shape the ankle-foot conforms to during most of the stance phase of gait. It can be used to describe both prosthetic ankle-feet (left) and natural ankle-feet (right) and is based on the description of forward progression of the lower limb as an inverted pendulum with a rocker-bottom over which the body rolls, like a wheel.....	7
Figure 5	The radius of curvature (length of the blue line) of the roll-over shape has been shown repeatedly to be approximately 30% of leg length. ....	8
Figure 6	Two prosthetic feet with seemingly dissimilar roll-over shapes that prove identical, apart from orientation, when overlain one atop the other.....	9
Figure 7	Ankle angle, moment, and power during stance. The period of stance over which roll-over shape is calculated (shaded yellow) does not include the period of late stance, during which a positive burst of ankle power occurs (highlighted red).....	10
Figure 8	A 6 degrees-of-freedom marker set was used to track lower extremity motion in the right-handed laboratory coordinate system.....	15
Figure 9	Ankle, foot-to-floor, and shank angle definitions. Figure adapted from <a href="http://www.istockphoto.com/photo/foot-bones-side-view-18523806">http://www.istockphoto.com/photo/foot-bones-side-view-18523806</a> .....	16

Figure 10	Sagittal plane kinematic model of shank progression used to predict ankle and knee joint center trajectories during the stance phase of gait. Figure adapted from <a href="http://www.istockphoto.com/photo/foot-bones-side-view-18523806">http://www.istockphoto.com/photo/foot-bones-side-view-18523806</a> . .....	18
Figure 11	Segmental power tracks the flow of mechanical power through a segment. Net segmental power of the shank is defined as the sum of muscle moment powers (red) and joint force powers (blue) occurring at the proximal and distal ends of the segment. ....	20
Figure 12	Observed and model-based sagittal plane shank trajectory, colored by rocker, during stance for one representative participant walking at 0.8 BH/s.....	24
Figure 13	Representative data depicting the interplay between motion capture-derived ankle, normalized foot-to-floor, and shank angles (solid lines) and model-based shank angle (dashed black line) during stance at walking speed 0.8 BH/s. Positive angles represent ankle dorsiflexion and a reclined shank. ....	25
Figure 14	Representative data for model-based (dashed lines) and motion capture-derived (solid lines) knee joint center (a) horizontal trajectory and (b) vertical trajectory during stance at walking speed 0.8 BH/s.....	27
Figure 15	Sagittal plane shank trajectory during stance, colored by rocker, with the shank segments during the forefoot and toe rockers extended downwards (pink lines). Calculations of the perpendicular distance of approximation ( <i>PDA</i> , inset) were made between the pivot point (purple) and the extended shank segments.....	28
Figure 16	Representative data for shank net segmental power (blue) and rate of energy change (red) during stance at walking speed 0.8 BH/s. ....	30
Figure 17	Visual representation of data for segmental power of the shank at peak ankle power (90% of stance) for one representative participant at walking speed 0.8 BH/s. The shank received 6.48 W/kg via the distal joint force power and released 1.99 W/kg via the proximal joint force power. ....	31

Figure 18	The telescoping shank was computed by collapsing all forefoot and toe rocker ankle positions to a pivot point (purple); fitting an exponential function to the distance between the collapsed knee joint center trajectory (gray and green lines) and the natural knee joint center trajectory (red trace); and elongating the shank based on the calculated exponential function to mimic the natural knee joint center trajectory.....	32
Figure 19	Representative plot of telescoping distance and exponential fit during the forefoot and toe rockers of stance at walking speed 0.8 BH/s. For this participant, telescoping distance was equal to $0.0015e^{0.079t} - 1$ .....	33
Figure 20	Distal shank telescoping power (blue) and distal shank joint force power (red) during stance for one representative participant at walking speed 0.8 BH/s.....	35
Figure 21	Proximal shank telescoping power (blue) and proximal shank joint force (red) power during stance for one representative participant at walking speed 0.8 BH/s.....	36
Figure 22	Model data for mean sagittal plane shank trajectory during stance at walking speed 0.8 BH/s with an ankle fixed in neutral alignment, colored by rocker. The height of the knee joint center drops off dramatically during the toe rocker (green lines). ....	39
Figure 23	Bland-Altman plots at heel strike. Data points are plotted with participant numbers. Solid lines represent the mean difference between measured and modeled values. Dashed lines represent the limits of agreement (mean $\pm$ 1.96 standard deviations). ....	52
Figure 24	Bland-Altman plots at foot flat. Data points are plotted with participant numbers. Solid lines represent the mean difference between measured and modeled values. Dashed lines represent the limits of agreement (mean $\pm$ 1.96 standard deviations). ....	53
Figure 25	Bland-Altman plots at heel off. Data points are plotted with participant numbers. Solid lines represent the mean difference between measured and modeled values. Dashed lines represent the limits of agreement (mean $\pm$ 1.96 standard deviations). ....	54

Figure 26	Bland-Altman plots at maximum dorsiflexion. Data points are plotted with participant numbers. Solid lines represent the mean difference between measured and modeled values. Dashed lines represent the limits of agreement (mean $\pm$ 1.96 standard deviations). .....	55
Figure 27	Bland-Altman plots at toe off. Data points are plotted with participant numbers. Solid lines represent the mean difference between measured and modeled values. Dashed lines represent the limits of agreement (mean $\pm$ 1.96 standard deviations). .....	56

## **ABSTRACT**

Individuals with transtibial amputation depend on prosthetic ankle-feet to ambulate. However, even today's state-of-the-art energy-storing-and-returning and bionic ankle-feet fail to replicate all the functions of the natural system. This deficiency may be due in part to the difficulty in analyzing prosthetic systems using traditional methods. Roll-over shape, the geometry the ankle-foot deforms to during stance, has been proposed as an improved characterization method. While useful, roll-over shape does not account for the period of late stance, during which important propulsive functions occur. Shank progression – the kinematics (translation and rotation) and energetics (flow of segmental power) of the lower leg – may provide a more complete description of ankle-foot function, including push-off. The overall purpose of the present study was to fully characterize the kinematics and energetics of shank progression during the stance phase of typical gait and to develop and evaluate alternate means of reproducing natural shank progression. Analyses were performed on an existing database of ten adult participants who completed overground instrumented gait analysis at a normal walking velocity. Shank kinematics were characterized by rotation and translation about an apparent virtual fixed ankle position. Power entered and exited the shank via the distal and proximal joint force terms, respectively. These data provided evidence for the design of a novel, non-biomimetic prosthetic shank capable of replicating shank kinematics and energetics via a “telescoping” (elongating) inverted pendulum mechanism. Such a device could lead to improved functional outcomes for prosthetic users in the future.

## Chapter 1

### INTRODUCTION AND SPECIFIC AIMS

Gait is the primary means of human locomotion beginning, on average, at one year of age (Capute et al., 1985). A full gait cycle is comprised of a stance phase and a swing phase, which account for about 60% and 40% of the cycle, respectively. The stance phase can be further subdivided into four successive “rockers,” which are denoted by the anatomical landmarks about which the foot and shank (lower leg) pivot (Figure 1) (Perry, 2010). In typical gait, the heel rocker initiates the gait cycle from heel strike through loading response (foot flat) and is preceded by the ankle rocker during midstance (foot flat to heel off), the forefoot rocker during terminal stance (heel off to maximum ankle dorsiflexion), and the toe rocker during pre-swing (maximum ankle dorsiflexion to toe off) (Perry, 2010).

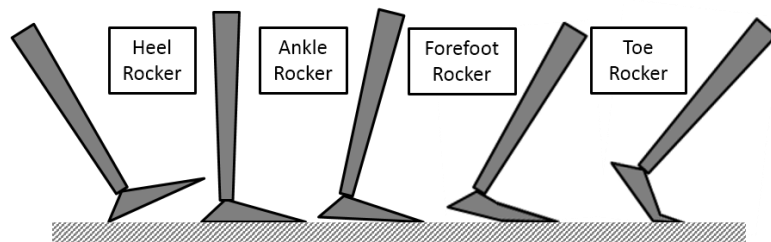


Figure 1 The stance phase of gait can be subdivided into four rockers, denoted by the anatomical landmarks about which the foot and shank pivot.

The natural ankle-foot is a complex network of bones, muscles, tendons, and ligaments. During the stance phase of gait, the ankle-foot serves as the interface

between the human body and the earth. It is responsible for a vast array of kinematic and energetic tasks, including maintenance of upright support, generation of forward propulsion of the body, initiation of leg swing, and absorption and production of energy (Winter, 1983; Hof et al., 1992; Kepple et al., 1997; Neptune et al., 2001). In fact, the natural ankle does more work than any other joint in the body during gait (Winter, 1983).

The kinematic features of the ankle-foot system can be described by rotations and translations of the foot (defined as the line from the second metatarsal head to the ankle joint center) and shank (ankle joint center to knee joint center) segments. These rotations and translations occur predominantly in the sagittal plane and arise from changes in the foot-to-floor angle and the ankle (shank relative to foot) angle (Figure 2) (Visual3D Wiki, 2015). Previous ankle-foot and walking models have also confined their analyses to the sagittal plane (Srinivasan et al., 2008; Ren et al., 2010; McGeer, 1990).

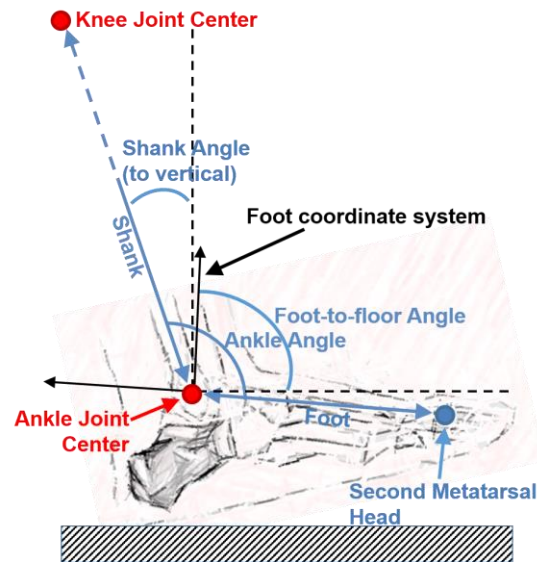


Figure 2 The kinematics (rotations and translations) of the foot and shank arise from the interplay between the foot-to-floor and ankle angles. Figure adapted from <http://www.istockphoto.com/photo/foot-bones-side-view-18523806>.

The energetics of the system can be described by net segmental powers. Power, of course, is the rate at which work is done. Segmental powers track the directional dynamics of energy flow into and out of segments and correspond to changes in mechanical energy of the segments (Winter, 2009). Net segmental power is defined as the sum of muscle moment powers and joint force powers, which both occur at the proximal and distal ends of segments. Muscle moment powers represent the active addition or subtraction of energy to the segment via concentric, eccentric, and isometric contractions. They are calculated by the scalar product of the joint moment and the joint angular velocity. Joint force powers represent the passive transfer of energy across joints to adjacent segments through the translational movement of the joints. They are calculated by the scalar product of the joint reaction force and the translational velocity of the joint center (Robertson & Winter, 1980)

(Figure 3). Positive segmental power terms indicate the rate of energy flow into the segment; negative values correspond to outflows of power from the segment.

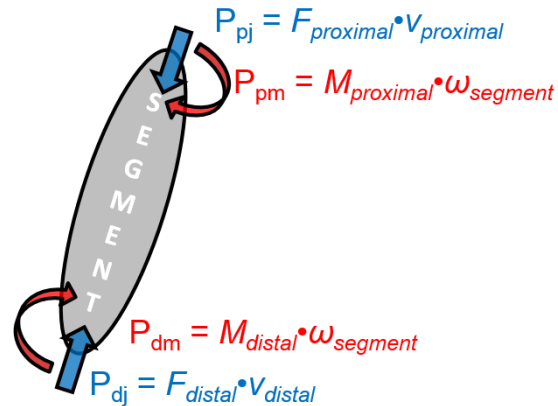


Figure 3 The energetics of a segment can be described by the flow of power into and out of its distal and proximal ends via muscle moment powers (red) and joint force powers (blue).

For individuals with transtibial amputation (limb loss below the knee), however, the natural ankle-foot structures are conspicuously absent. These individuals rely instead on prosthetic ankle-feet in order to reproduce the kinematic and energetic features of gait. Fortunately, the degree to which prostheses mimic the functions of the natural ankle-foot has improved dramatically since early designs, which filled only basic functional and cosmetic roles (Gutfleisch, 2003; Hafner et al., 2002b). The 1980's in particular saw the advent of energy-storing-and-returning devices. These prostheses improved functional mobility and performance considerably by storing energy in early stance and returning it in late stance in a non-biomimetic fashion (Nielsen et al., 1989). Still, even today's most state-of-the-art energy-storing-and-returning prostheses are unable to match human performance in all of the above-

mentioned tasks for which the natural ankle-foot are responsible. Due to limited plantar flexion, power generation as walking speed increases remains one of the greatest design challenges for unpowered prostheses (Hafner et al., 2002a; Hansen, Childress, Miff, et al., 2004; Cherelle et al., 2014; Sanderson & Martin, 1997). The result of this shortcoming is an increase in metabolic cost compared to typical (Versluys et al., 2009), as well as gait asymmetry and compensatory patterns throughout the kinetic chain (Winter & Sienko, 1988; Nielsen et al., 1989; Silverman et al., 2008; Isakov et al., 2000).

Bionic, or powered, ankle-feet have been proposed as a possible solution to the power generation issue. These devices simulate ankle plantar flexion, thereby providing a more human-like push-off (Cherelle et al., 2014). The downside to powered prostheses, however, is their mass. Because moment of inertia (resistance to rotational motion) increases in proportion to the square of the distance of the load from its axis of rotation, the added power generation comes at the cost of a bulky distal load. As a result, these devices provide users no advantage for functional activities and actually introduce additional asymmetries to proximal joints compared to traditional energy-storing-and-returning prosthetic ankle-feet (Ferris et al., 2012).

In spite of the advances in technology, objective biomechanically-based guidelines for the optimal design, prescription, and customization of prosthetic ankle-feet are lacking (Hansen et al., 2000; Fey et al., 2011; Hafner et al., 2002a). When it comes to component selection, prosthetists are forced to rely on clinical experience and patient feedback (van der Linde et al., 2004; Fey et al., 2011; Fridman et al., 2003) to choose between dozens of minimally differentiable devices (Hafner et al., 2002a; Hafner et al., 2002b).

The lack of objective guidelines may be due to the difficulty in describing the prosthetic ankle-foot using traditional methods. Energy-storing-and-returning prosthetic ankle-feet store and release energy through material deformation and elastic recoil. As such, the assumptions of rigid bodies and fixed axes of rotation that are inherent to traditional inverse dynamics analyses are only loose approximations (Knox, 1996; Geil et al., 2000), with errors propagating the further up the analysis travels from the ankle-foot. Studies of the energetic and mechanical properties of prosthetic ankle-feet are of limited predictive value, as they cannot determine exactly how an individual will perform with a particular device (Hafner et al., 2002b). The loading parameters in these studies also differ from those incurred during actual gait (Hansen, Childress, Miff, et al., 2004; Curtze et al., 2009).

Clearly, a more general characterization method of the ankle-foot that can be applied to both the natural and prosthetic systems is needed. Roll-over shape, or the effective geometry the ankle-foot conforms to during a portion of the stance phase of gait, has been proposed as one such method (Hansen et al., 2000) (Figure 4, left). Roll-over shape is calculated by transforming the center of pressure of the ground reaction force from the laboratory coordinate system to the shank coordinate system and curve-fitting the resulting arc (Hansen, Childress & Knox, 2004). It can be considered the cumulative effect of the heel, ankle, and forefoot rockers, where forward progression of the lower limb is described by an inverted pendulum with a rocker-bottom over which the body “rolls” like a wheel (Gard & Childress, 2001) (Figure 4, right).

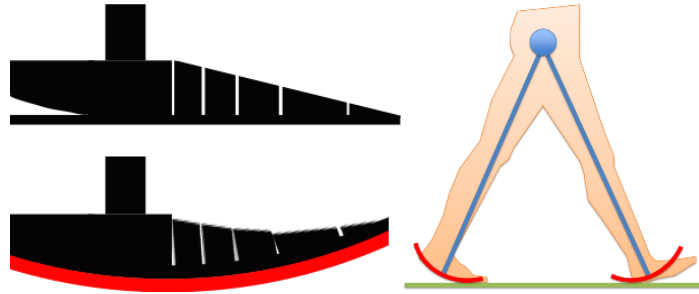


Figure 4 Roll-over shape (red arc) denotes the shape the ankle-foot conforms to during most of the stance phase of gait. It can be used to describe both prosthetic ankle-feet (left) and natural ankle-feet (right) and is based on the description of forward progression of the lower limb as an inverted pendulum with a rocker-bottom over which the body rolls, like a wheel.

The key parameter of interest for roll-over shape has historically been its effective radius of curvature during the portion of stance from heel strike to contralateral heel strike (Figure 5, blue line). Radius of curvature has repeatedly been shown to be approximately 30% of leg length (McGeer, 1990; Hansen, Childress, Miff, et al., 2004). Remarkably, multiple studies have confirmed the radius of curvature's invariance to changes in walking velocity, added carrying loads, shoe heel height, and shoe rocker-bottom radius (Hansen & Childress, 2010), which makes it a simple and attractive criterion for the analysis and design of prosthetic ankle-feet. After contralateral heel strike, the transformed center of pressure does not conform to the same circular shape and is excluded from the analysis.

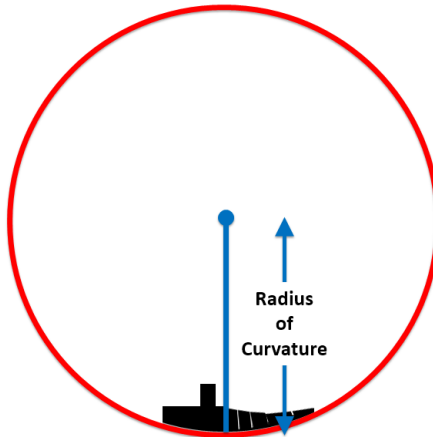


Figure 5 The radius of curvature (length of the blue line) of the roll-over shape has been shown repeatedly to be approximately 30% of leg length.

In the earliest application of roll-over shape to prostheses, a rigid rocker model was applied to a solid ankle cushioned heel (SACH) foot (Stein & Flowers, 1987). Although “roll-over shape” has become a buzzword for prosthetics companies, the radius of curvature has, in fact, successfully aided the design of numerous recent prosthetic ankle-feet (Curtze et al., 2009). A field study in an underdeveloped country reported improved performance and functionality over traditional components with the low-cost Shape&Roll Prosthetic Foot. Users exhibited a widened range of walking speeds (both faster and slow), ability to traverse longer distances, and reduced perceived exertion compared to their SACH feet. However, step length asymmetry continued to prove problematic, perhaps due to a reduced functional foot length compared to typical (Meier et al., 2004).

While clearly a useful metric, roll-over shape it is not without its deficiencies, especially in terms of application to the amputee population. It has been shown that humans modulate their muscular torque output in order to maintain a consistent roll-over shape, likely because it is energetically advantageous to do so (Adamczyk et al.,

2006). However, the precise mechanism underlying this consistent roll-over shape is not well understood. It may be that individuals with transtibial amputation are unable to replicate the muscle coordination patterns that result in the invariant shape (Hansen & Childress, 2010). Moreover, due to the prosthetic system's decreased work output capability, as well as an increased need for stability and balance, Hansen & Childress hypothesize that the optimal radius of curvature for a prosthetic ankle-foot may actually be larger (i.e. "flatter") than typical. In addition, traditional roll-over shape descriptions fail to take into account both arc length, a key determinant of step length symmetry, and orientation. For example, two prosthetic feet could have identical roll-over shapes but more dorsiflexed or plantar flexed orientations (Figure 6) (Hansen & Childress, 2010).

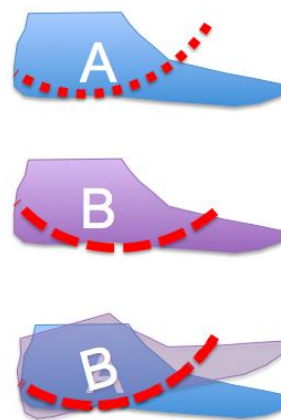


Figure 6 Two prosthetic feet with seemingly dissimilar roll-over shapes that prove identical, apart from orientation, when overlain one atop the other

Finally, roll-over shape is a kinematic representation only, with no description of the kinetics or energetics of the ankle-foot. Because roll-over shape is calculated only from heel strike to contralateral heel strike, it fails to provide any quantification of late

stance – a full 17% of stance (Perry, 2010) and the interval over which prosthetic ankle-feet return energy (Knox, 1996) and natural peak ankle power occurs (Figure 7, highlighted in yellow).

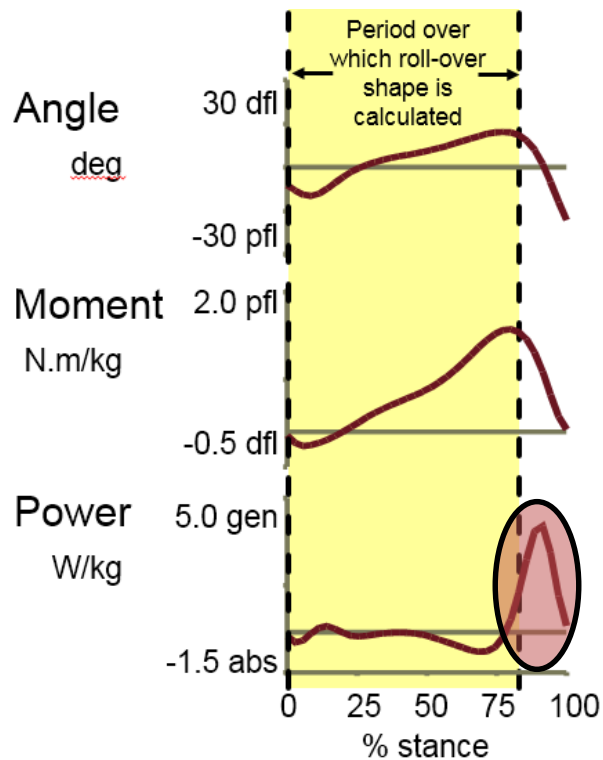


Figure 7 Ankle angle, moment, and power during stance. The period of stance over which roll-over shape is calculated (shaded yellow) does not include the period of late stance, during which a positive burst of ankle power occurs (highlighted red).

In sum, the description that roll-over shape provides of the ankle-foot system is incomplete. Replicating typical kinematics of the shank, on the other hand, has been shown to correct the kinematics of the proximal segments (the thigh, pelvis, trunk, and even head) accordingly, as well as the alignment of the ground reaction force relative to the knee and hip, an essential feature for minimizing the neuromuscular cost of

walking (Owen, 2004). Thus, an approach that characterizes the kinematics and also the energetics of the shank during the stance phase of gait is warranted. The overall purpose of the present study was to fully characterize the kinematics and energetics of shank progression during the stance phase of typical gait and to develop and evaluate alternate means of reproducing natural shank progression. The following three specific aims were proposed:

**Aim 1.** Develop and validate a sagittal plane kinematic model of shank progression during the stance phase of gait.

**Hypothesis 1A.** There would be a strong correlation between the model-based and motion capture-derived shank angle in the laboratory coordinate system.

**Hypothesis 1B.** There would be strong correlations between the model-based and motion capture-derived knee joint center positions.

**Aim 2.** Conduct an energetics analysis of shank progression during the stance phase of gait via distal and proximal net segmental power flows into and out of the shank in order to quantify “push-off.”

**Aim 3.** Develop and evaluate a sagittal plane model of a “telescoping” prosthetic shank during the stance phase of gait that could be used to replicate typical shank kinematics and energetics.

**Hypothesis 3A.** There would be a strong correlation between the anatomical and model-based knee joint center trajectories.

**Hypothesis 3B.** There would be a strong correlation between the anatomical and model-based distal shank powers.

**Hypothesis 3C.** There would be a strong correlation between the anatomical and model-based proximal shank powers.

## **Chapter 2**

### **RESEARCH STRATEGY**

#### **2.1 Significance**

There are nearly 2 million individuals with amputation in the United States alone (NLLIC, 2007), and this number could as much as double by the year 2050 (Ziegler-Graham et al., 2008). With the cost of assistive devices numbering in the tens of thousands of dollars (Blough et al., 2010), the toll on the healthcare system is considerable. Yet even today's state-of-the-art prostheses fail to provide users with the levels of function they desire. In fact, though extremely costly, the latest bionic (powered) devices actually perform the same as traditional energy-storing-and-returning prosthetic ankle-feet on functional activities and introduce additional asymmetries to proximal joints during gait (Ferris et al., 2012). As such, a new paradigm of care is needed – one that seeks to improve functional outcomes for individuals with amputation who seek high levels of function while simultaneously reducing the cost of care. This paradigm may be based on prosthetic designs that assist gait via a novel, nontraditional approach.

#### **2.2 Innovation**

In typical gait, the ankle plantar flexors are known to provide push-off in late stance to propel the body forward (Neptune et al., 2001). However, individuals with transtibial amputation wearing energy-storing-and-returning prosthetic ankle-feet lack much of this crucial source of propulsion (Cherelle et al., 2014; Sanderson & Martin,

1997). In recent years, prosthetic ankle-feet have been designed to mimic roll-over shape (Hansen et al., 2000). However, a biomimetic radius of curvature alone does not address several key components of stance, including the kinematics of proximal segments, ankle-foot kinetics, and push-off energetics. The latest powered prostheses seek to restore ankle push-off energetics in a biomimetic fashion but do so at the cost of a bulky distal load, which results in proximal compensations. This study provides a highly innovative approach for evaluating the kinematics and energetics of shank progression. These findings have led to a novel, non-biomimetic approach to reproducing stance-phase shank kinematics and energetics based on a “telescoping” (elongating) inverted pendulum (TIP) shank model. This novel design could lead to improved functional outcomes for individuals with lower extremity amputation.

## 2.3 Approach

### 2.3.1 Participants

Data were drawn from an existing database of ten typical adult participants with no prior history of musculoskeletal disorder. Participants provided informed consent according to the Human Movement Analysis Database protocol approved by the Human Subject Review Board at the University of Delaware (Study Number 324555-1). The characteristics of the participants are summarized in Table 1.

Table 1 Participant characteristics

<b>Participant ID</b>	<b>Sex</b>	<b>Age (years)</b>	<b>Height (meters)</b>	<b>Body mass (kg)</b>	<b>Foot Length (m)</b>	<b>Shank Length (m)</b>
1	M	28	1.77	75.0	0.154	0.410
2	M	27	1.78	81.0	0.160	0.436

3	M	24	1.76	81.0	0.158	0.412
4	M	23	1.84	74.5	0.166	0.407
5	F	21	1.71	53.5	0.137	0.397
6	F	23	1.63	62.6	0.144	0.389
7	F	22	1.64	60.0	0.142	0.376
8	F	29	1.67	59.5	0.149	0.395
9	F	20	1.65	62.7	0.140	0.376
10	F	25	1.64	86.5	0.149	0.371
Mean $\pm$ SD:	4 M; 6 F	24.2 $\pm$ 3.0	1.71 $\pm$ 0.07	69.6 $\pm$ 11.3	0.150 $\pm$ .009	0.397 $\pm$ 0.020

### 2.3.2 Data Collection

Participants underwent fully instrumented gait analysis with a 6 degrees-of-freedom marker set to track lower extremity motion (Figure 8) (Holden & Stanhope, 1998). Kinematic data were collected from the right (dominant) lower extremity using a six-camera motion capture system (Motion Analysis Corp., Santa Rosa, CA). Participants walked barefoot over a strain gauge force platform embedded along a straight-line walkway (AMTI, Watertown, MA, USA). Participants walked at a normal scaled velocity of 0.8 body heights (BH) per second for a minimum of two trials (Rosenrot et al., 1980). Speed was verified with two photocell beams located 3 meters apart. Participants rested as needed. A right-handed laboratory coordinate system was established with the positive x-axis directed to the participant's right, the positive y-axis in the direction of forward progression, and the positive z-axis up (Figure 8).

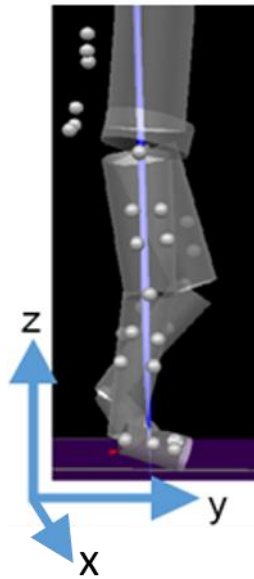


Figure 8 A 6 degrees-of-freedom marker set was used to track lower extremity motion in the right-handed laboratory coordinate system.

### 2.3.3 Data Processing, Definitions, and Analysis

Data were processed using Visual3D software (C-Motion Inc., Germantown, MD). Kinematic data were sampled at 240 Hz in order to identify the precise location of the stance-phase gait events of heel strike, foot flat, heel off, maximum ankle dorsiflexion, and toe off (see Table 2 for definition of events). The ankle angle was defined by the angle between the shank segment (ankle joint center to knee joint center) and the foot segment (second metatarsal head to ankle joint center). Dorsiflexion corresponded to a positive ankle angle. Foot-to-floor angle was defined by the rotation of the foot coordinate system relative to the laboratory coordinate system, with foot flat corresponding to an angle of approximately  $+70^\circ$ . Shank angle was measured from vertical, where a reclined position (i.e. the position of the shank at heel strike) corresponded to a positive angle (See Figure 9). Force plate data were sampled at 1200 Hz. The raw kinematic and kinetic data were low-pass filtered at cut-

off frequencies of 6 Hz and 25 Hz, respectively, using a zero-lag fourth-order Butterworth filter. Data analysis was performed using custom scripts in Visual3D and Mathematica (Wolfram Research Inc., Champaign, IL).

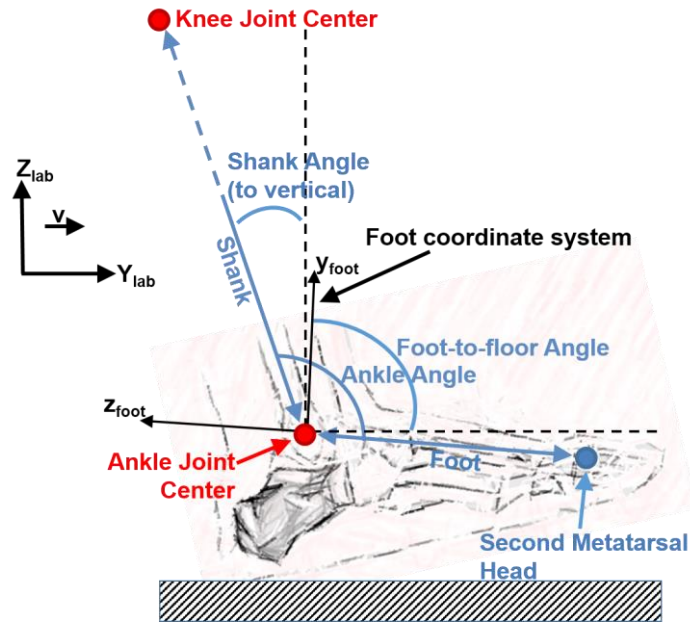


Figure 9 Ankle, foot-to-floor, and shank angle definitions. Figure adapted from <http://www.istockphoto.com/photo/foot-bones-side-view-18523806>.

Table 2 Definition of stance-phase gait event placement

Gait Event	Definition
Heel strike	Ground reaction force exceeded 20 N
Foot flat	Vertical velocity of distal end of foot (second metatarsal head) approached 0 m/s
Heel off	Foot-to-floor angle increased $0.5^\circ$ from its value when the height of the ankle joint center was at its minimum
Maximum ankle dorsiflexion	Ankle angle reached maximum value
Toe off	Ground reaction force fell below 20 N

## 2.3.4 Kinematics of Shank Progression

### 2.3.4.1 Kinematic Model

To describe the kinematics of shank progression, the rotation and translation of the shank and foot were measured during each rocker of stance as well as over the entire stance phase. To average across trials and participants, the horizontal position of the ankle was set to zero at heel strike for all walking trials. The percentages of shank rotation attributable to the ankle and foot-to-floor angles were also calculated by dividing these angles by the shank angle.

To determine the mathematical relationships between foot and ankle rotation and shank rotation and translation, a sagittal plane kinematic model was developed (Figure 10). Given the angles of the foot and ankle, the lengths of the foot and shank, and the position of the distal end of the foot (defined by the second metatarsal head), the kinematic model predicted shank angle and the positions of the distal and proximal ends of the shank (defined by the ankle and knee joint centers) in the laboratory coordinate system:

$$y_{ankle} = y_{MH2} - \sin(\theta) * L_{foot} \quad (3.1)$$

$$z_{ankle} = z_{MH2} + \cos(\theta) * L_{foot} \quad (3.2)$$

$$y_{knee} = y_{ankle} - \sin(\theta_0 - \varphi) * L_{shank} \quad (3.3)$$

$$z_{knee} = z_{ankle} + \cos(\theta_0 - \varphi) * L_{shank} \quad (3.4)$$

where  $L_{foot}$  and  $L_{shank}$  are the lengths of the foot and shank, respectively;  $MH2$  refers to the position of the second metatarsal head;  $\theta$  corresponds to the foot-to-floor angle;  $\theta_0$  represents the foot-to-floor angle normalized to  $0^\circ$  in the static pose (quiet standing, feet flat on floor);  $\varphi$  is the ankle (shank-to-foot) angle; and the quantity  $\theta_0 - \varphi$  yields the shank angle relative to the vertical (z-)axis of the lab. To validate the model, the

calculated shank angle and knee joint center were compared to the motion captured-derived values.

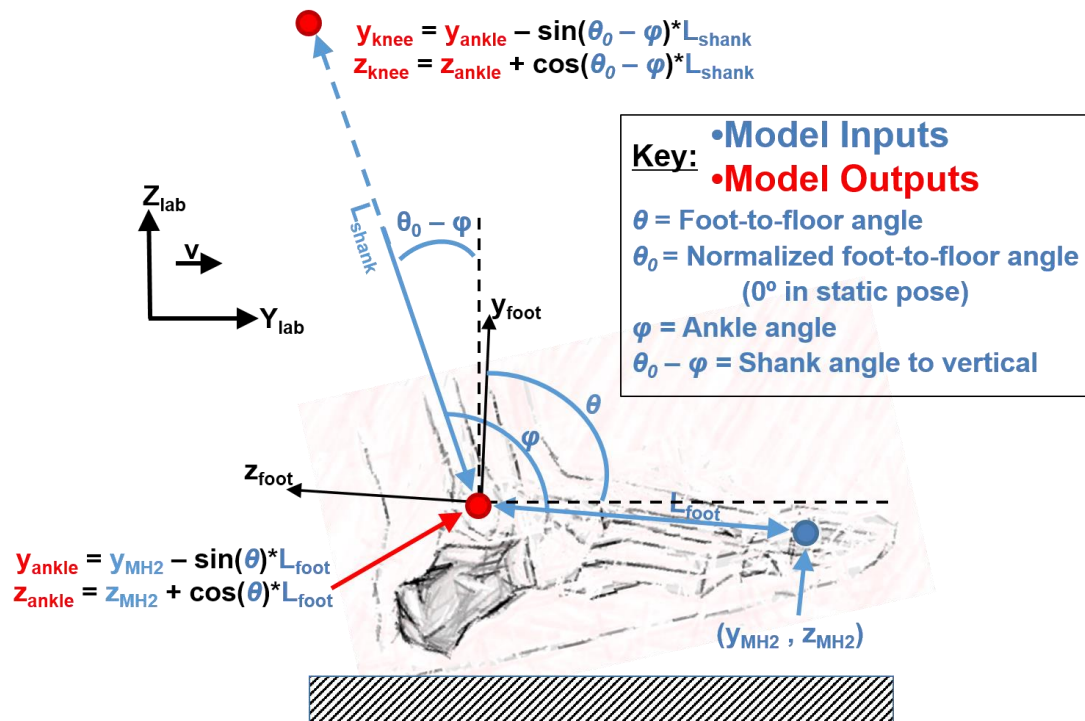


Figure 10 Sagittal plane kinematic model of shank progression used to predict ankle and knee joint center trajectories during the stance phase of gait. Figure adapted from <http://www.istockphoto.com/photo/foot-bones-side-view-18523806>.

### 2.3.4.2 Point of Rotation

A virtual fixed position, or “pivot point,” about which the shank segments rotated during the forefoot and toe rockers of stance was estimated at the location of the ankle joint center at the termination of the ankle rocker (immediately prior to the gait event of heel off). To determine the validity of this choice of a pivot point, the forefoot and toe rocker segments were extended backwards and down, and the

perpendicular distances between the pivot point and the extensions of the shank segment were calculated.

### 2.3.5 Energetics of Shank Progression

In accordance with the principles laid out by Robertson & Winter, the flow of mechanical power into and out of the distal and proximal shank was used to quantify the sagittal plane push-off energetics of the shank during late stance (Robertson & Winter 1980) (Figure 11). The net segmental power of the shank ( $P_{shank}$ ) was calculated as the sum of the proximal muscle power ( $P_{pm}$ ), proximal joint force power ( $P_{pj}$ ), distal muscle power ( $P_{dm}$ ), and distal joint force power ( $P_{dj}$ ) of the shank:

$$P_{shank} = P_{pm} + P_{pj} + P_{dm} + P_{dj} \quad (3.5)$$

$$= M_{proximal} \cdot \omega_{shank} + F_{proximal} \cdot v_{proximal} + M_{distal} \cdot \omega_{shank} + F_{distal} \cdot v_{distal}$$

where  $M_{proximal}$  and  $M_{distal}$  are the moments applied to the shank about the medio-lateral x-axis at the proximal and distance ends;  $F_{proximal}$  and  $F_{distal}$  are the joint reaction forces applied to the proximal and distal ends of the shank;  $v_{proximal}$  and  $v_{distal}$  are the translational velocities of the proximal and distal ends of the shank; and  $\omega_{shank}$  is the angular velocity of the shank about the x-axis of the lab. Positive terms indicate the rate of energy flow into the segment; negative values correspond to outflows of power from the segment. To quantify “push-off,” the direction and magnitude of the segmental power component terms were evaluated at the point at which the ankle joint power reached its peak during late stance.

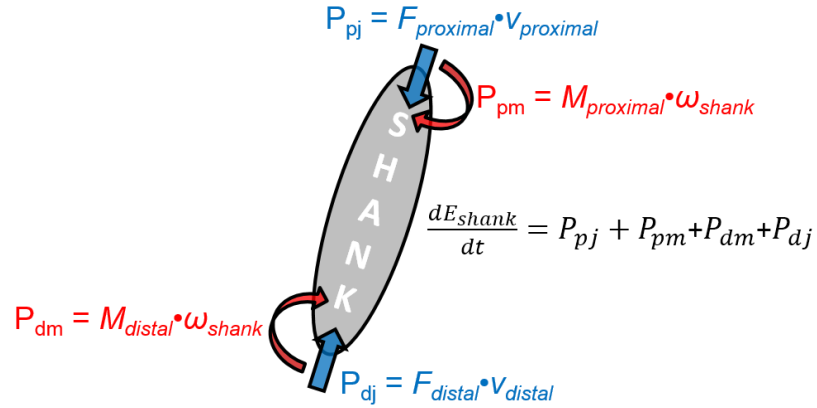


Figure 11 Segmental power tracks the flow of mechanical power through a segment. Net segmental power of the shank is defined as the sum of muscle moment powers (red) and joint force powers (blue) occurring at the proximal and distal ends of the segment.

### 2.3.5.1 Validation of Net Segmental Power

In order to assess the validity of the segmental power terms, the rate of change of energy of the shank segment was compared to the net segmental power (Siegel et al., 1996). Theoretically, by the work energy theorem,

$$\frac{dE_{shank}}{dt} = P_{shank} \quad (3.6)$$

However, discrepancies may exist due to the restriction of the model to the sagittal plane (Robertson & Winter, 1980; Siegel et al., 1996). The total mechanical energy of the shank ( $E_{shank}$ ) was calculated as the sum of the potential energy ( $PE$ ), translational kinetic energy ( $TKE$ ), and rotational kinetic energy ( $RKE$ ):

$$\begin{aligned} E_{shank} &= PE + TKE + RKE \\ &= mgz_{cm} + \frac{1}{2}m\vec{v}_{cm}^2 + \frac{1}{2}I\omega_{shank}^2 \end{aligned} \quad (3.7)$$

where  $z_{cm}$  is the height of the center of mass of the shank,  $v_{cm}$  is the sagittal plane translational velocity of the shank,  $I$  is the moment of inertia of the shank about the segment's x-axis through its center of gravity, and  $\omega_{shank}$  is the angular velocity of the

shank about the x-axis of the lab. The rate of energy change at the  $i^{\text{th}}$  percent of stance ( $dE/dt_i$ ) was calculated as the centered finite difference of the energy:

$$\frac{dE}{dt_i} = \frac{E_{i+1} - E_{i-1}}{2\Delta t} \quad (3.8)$$

where  $\Delta t$  is the change in time between adjacent percentages of stance.

### 2.3.6 Telescoping Inverted Pendulum Shank Model

A telescoping inverted pendulum (TIP) model of the shank was used to explore the feasibility of reproducing the kinematics and energetics of natural shank progression via a non-biomimetic approach. With the angular orientation of the shank preserved, all shank segments for the forefoot and toe rockers were collapsed to emanate from the “pivot point” established through the methods described in Section 2.3.4.2. Elongation of the telescoping shank model was accomplished following an exponential function, where the constants of the function were determined by the distance from the now “collapsed knee joint center position” to the original trajectory. The maximum telescoping distance corresponded to the distance the shank elongated at toe off. To assess the validity of the model from a kinematic standpoint, the trajectory of the proximal end of the telescoping shank was compared to the natural knee joint center trajectory.

#### 2.3.6.1 Telescoping Shank Powers

To determine the extent to which the energetics of the TIP shank model could replicate natural shank progression energetics, telescoping shank powers were calculated and compared to observed natural shank segmental powers. Distal shank telescoping power ( $P_{telescoping\ distal}$ ) due to the telescoping effect was calculated as

$$P_{telescoping\ distal} = F_{GRF} \bullet v_{telescoping} \quad (3.9)$$

where  $F_{GRF}$  was the sagittal plane ground reaction force and  $v_{telescoping}$  the telescoping velocity, as determined by differentiating the telescoping distance. Proximal shank telescoping power ( $P_{telescoping\ proximal}$ ) was calculated as

$$P_{telescoping\ proximal} = F_{JRF} \bullet v_{telescoping\ knee} \quad (3.10)$$

where  $F_{JRF}$  represents the observed joint reaction force at the knee during typical gait  $v_{telescoping\ knee}$  is the trajectory of the telescoping knee.

### 2.3.7 Statistical Analysis

Gait data for each participant were based on averaged, time-normalized stance phases of gait (101 points) extracted from between 2 and 4 gait cycles. In order to discretize the data for comparison of model and motion capture-derived values, data values were extracted at each of the five gait events corresponding to the rockers of stance (heel strike, foot flat, heel off, maximum dorsiflexion, and toe off). Agreement between all model-based and motion capture-derived values was determined by Bland-Altman mean differences and limits of agreement (mean  $\pm$  1.96 standard deviations of comparison data minus model data) (Bland & Altman, 1986). Intraclass correlations (ICC (3,2)) were also calculated at each of the five gait events for reliability (Weir, 2005). Overall agreement and correlation for each variable were determined by averaging across gait events. The models were deemed accurate for moderate to high intraclass correlations to the motion capture-data (ICC > 0.80).

## **Chapter 3**

### **RESULTS**

Bland-Altman mean differences and limits of agreement, along with intraclass correlations (ICC (3,2)), between model-based and motion capture-derived values at each of the five gait events corresponding to the four rockers of stance (heel strike, foot flat, heel off, maximum dorsiflexion, and toe off) are provided in Appendix A. Almost all participant data fell within the limits of agreement, were randomly dispersed, and exhibited no trends. Means across all five gait events for all 10 participants are presented below.

#### **3.1 Kinematics of Shank Progression**

In order to determine the mathematical relationships between foot and ankle rotation and shank progression (rotation and translation) during the stance phase of gait, a sagittal plane kinematic model was developed. (See Section 2.3.4 for a description of the model). The model predicts shank angle and the positions of the distal and proximal ends of the shank (defined by the ankle and knee joint centers, respectively). Figure 12 depicts a representative observed sagittal plane shank trajectory during the stance phase of gait, colored by the four rockers, as well as the model-based ankle and knee joint center trajectories (overlaid in red). The interplay of foot and ankle rotation appeared to result in shank behavior equivalent to a “launching inverted pendulum” during the forefoot and toe rockers.

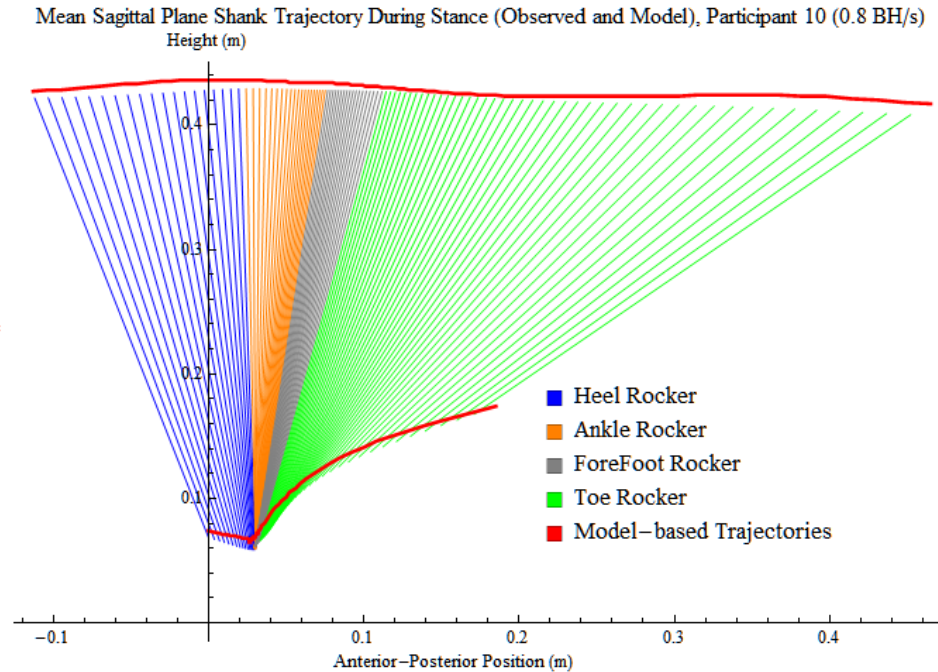


Figure 12 Observed and model-based sagittal plane shank trajectory, colored by rocker, during stance for one representative participant walking at 0.8 BH/s

### 3.1.1 Shank Angle

Shank rotation resulted from a combination of ankle and foot-to-floor rotation. Figure 13 depicts the interplay of the ankle angle, foot-to-floor angle, and shank angle (to vertical) during stance for one representative participant walking at 0.8 BH/s. Positive angles correspond to a dorsiflexed ankle and a “reclined” shank (i.e. the orientation of the shank at heel strike); negative angles denote a plantar flexed ankle and “inclined” shank. The model-based shank angle was calculated in the kinematic model as the mathematical difference between the normalized foot-to-floor angle and the ankle angle (Section 2.3.4.1) and is also drawn in Figure 13. Across all 10 participants and five gait events, the mean [limits of agreement] of the difference between the model-based and motion capture-derived shank angles was 0.655 [-2.474, 1.169] degrees with ICC (3,2) = 0.959.

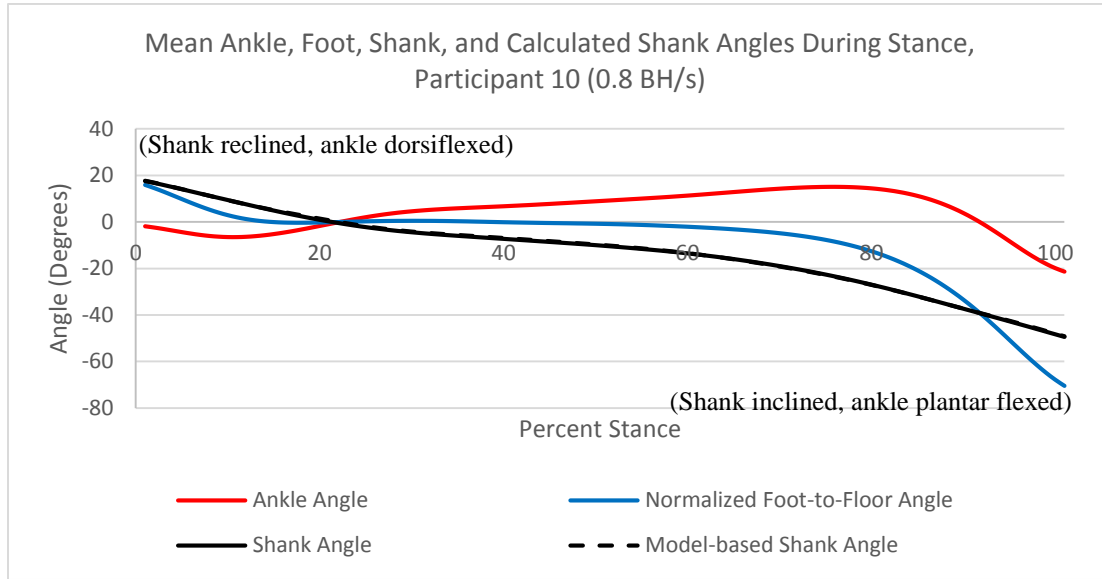


Figure 13 Representative data depicting the interplay between motion capture-derived ankle, normalized foot-to-floor, and shank angles (solid lines) and model-based shank angle (dashed black line) during stance at walking speed 0.8 BH/s. Positive angles represent ankle dorsiflexion and a reclined shank.

On average across all participants, the shank rotated through a total of  $55.48 \pm 4.83^\circ$  during stance. The excursions per rocker and total excursions over all of stance for the ankle, foot-to-floor, and shank angles are provided in Table 3. For a further breakdown of angular excursions for each participant, see Appendix A.

Table 3 Angular excursions by rocker, means and standard deviations

Angle	Heel Rocker (°)	Ankle Rocker (°)	Forefoot Rocker (°)	Toe Rocker (°)	Total (°)
Ankle	$1.75 \pm 1.39$	$11.03 \pm 2.67$	$4.15 \pm 2.30$	$-32.92 \pm 4.26$	$-15.99 \pm 6.39$
Foot-to-floor	$-16.03 \pm 3.09$	$-0.04 \pm 0.41$	$-5.66 \pm 1.42$	$-59.42 \pm 6.84$	$-81.16 \pm 8.11$
Shank	$-17.00 \pm 2.98$	$-0.04 \pm 0.41$	$-9.79 \pm 3.10$	$-28.65 \pm 3.20$	$-55.48 \pm 4.83$

The relative contributions of the ankle and foot-to-floor angles to shank rotation were calculated by dividing the respective angles by shank angle. Mean values over all participants are shown in Table 4. At heel strike, the reclined position of the shank was attributable to the foot-to-floor angle. At heel off, the shank began to incline due to ankle dorsiflexion. At toe off, inclination of the shank was due to foot-to-floor motion, while plantar flexion counteracted that rotation.

Table 4 Mean relative contributions across all participants of ankle and foot-to-floor angles to shank angle during stance at walking velocity 0.8 BH/s.

<b>Angle</b>	<b>Heel Strike</b>	<b>Foot Flat</b>	<b>Heel Off</b>	<b>Max Dorsiflexion</b>	<b>Toe Off</b>
Ankle angle	2%	--	92%	70%	-29%
Foot-to-floor angle	98%	--	8%	30%	129%

### 3.1.2 Shank Translation

Shank translation during the stance phase of gait was described by the horizontal (anterior-posterior) and vertical (superior-inferior) trajectory of its proximal endpoint, which was defined by the knee joint center. Figure 14 depicts this motion for one representative participant walking at 0.8 BH/s. Model-based trajectories (dashed lines), as determined by the kinematic model (Section 2.3.4.1), are overlaid atop the motion capture-derived ones (solid lines).

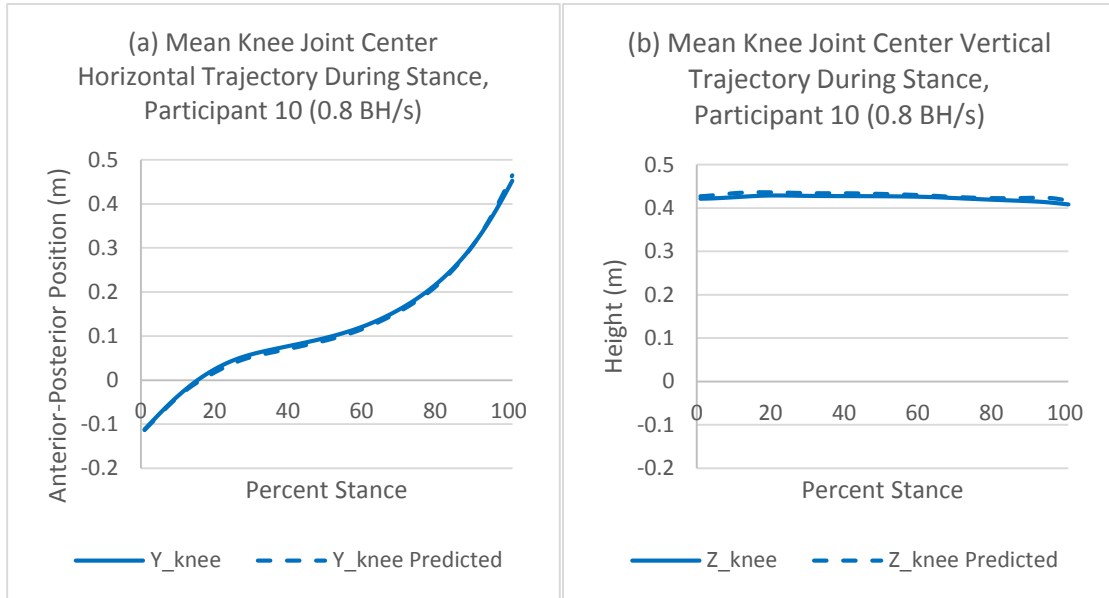


Figure 14 Representative data for model-based (dashed lines) and motion capture-derived (solid lines) knee joint center (a) horizontal trajectory and (b) vertical trajectory during stance at walking speed 0.8 BH/s.

Across all 10 participants and five gait events, the mean [limits of agreement] of the difference between the model-based and motion capture-derived horizontal knee joint center trajectory was 0.002 [-0.012, 0.014] meters with ICC (3,2) = 0.970. For the vertical knee joint center trajectory, the mean [limits of agreement] was 0.006 [-0.016, 0.004] meters with ICC (3,2) = 0.982. The vertical velocity of the knee joint center oscillated about 0 m/s for the majority of stance and reached a minimum just prior to toe off.

### 3.1.3 Pivot Point Approximation

To determine the validity of the selection of the pivot point as the approximate point about which rotation of the inverted pendulum shank occurred, the perpendicular distance of approximation (*PDA*) between the pivot point and downward extensions of

the shank were calculated by projecting the vector from the pivot point to a point on the extended shank ( $\vec{r}$ ) onto the vector perpendicular to the extended shank ( $\vec{v}$ ) (Figure 15):

$$PDA = |\hat{v} \cdot \vec{r}| \quad (3.12)$$

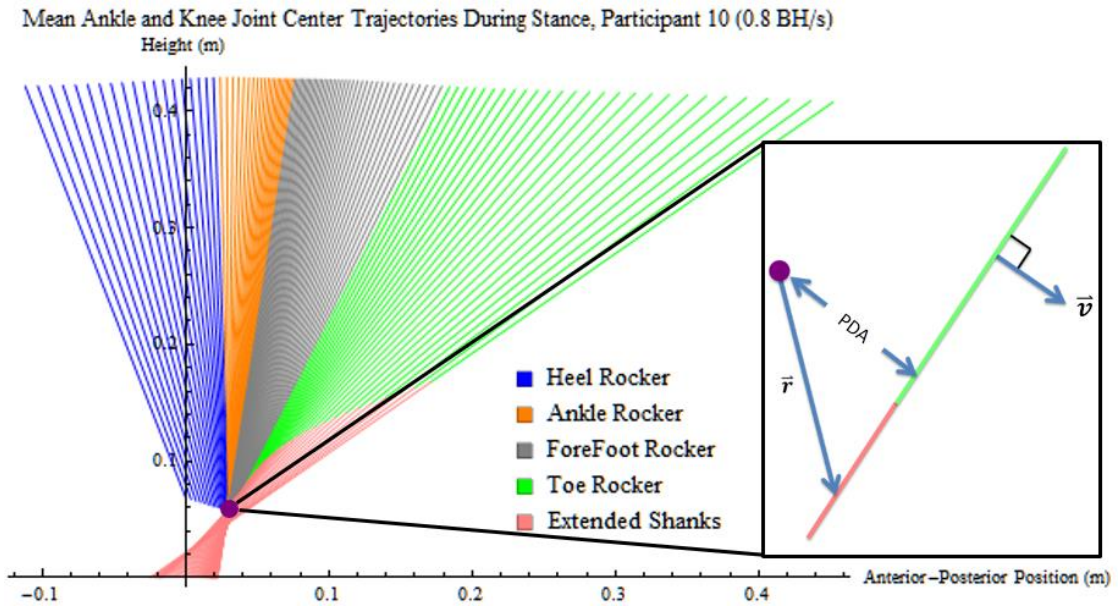


Figure 15 Sagittal plane shank trajectory during stance, colored by rocker, with the shank segments during the forefoot and toe rockers extended downwards (pink lines). Calculations of the perpendicular distance of approximation (*PDA*, inset) were made between the pivot point (purple) and the extended shank segments.

On average, the pivot point was within  $0.003 \pm 0.002$  m of the extended shank, with the largest mean distance of all participants being 0.009 m (Table 5).

Table 5 Mean perpendicular distance of approximation (*PDA*) for the pivot point

<b>Participant</b>	<b>Mean PDA (m)</b>
1	0.001
2	0.004
3	0.003
4	0.003
5	0.002
6	0.002
7	0.009
8	0.002
9	0.004
10	0.003
Mean $\pm$ SD:	0.003 $\pm$ 0.002

### **3.2 Energetics of Shank Progression**

To quantify the push-off energetics of the shank during late stance, the flow of mechanical power into and out of the distal and proximal ends of the shank was calculated using Robertson & Winter's segmental power techniques, as described in Section 2.3.5 (1980).

#### **3.2.1 Validation of Shank Net Segmental Power**

In order to assess the validity of the component segmental power terms, the rate of change of energy of the shank segment was compared to the net segmental power (Siegel et al., 1996) (Section 2.3.5.1). Figure 16 depicts the mean shank net segmental power and rate of change of energy of the shank for one representative participant walking at 0.8 BH/s. Across all 10 participants and five gait events, the mean [limits of agreement] of the difference between the shank segmental power and the rate of change of energy of the shank was 0.035 [-0.073, 0.087] W/kg with ICC (3,2) = 0.739. (See Appendix A for breakdown by gait event.)

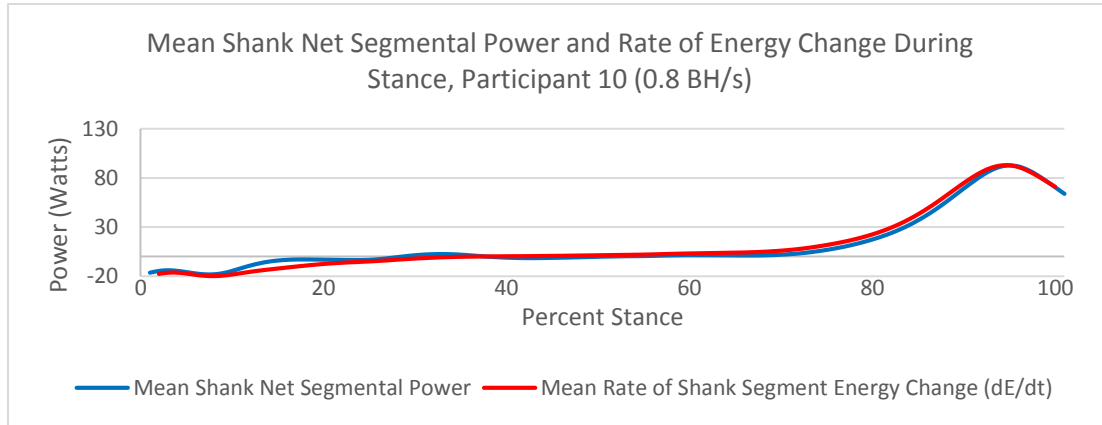


Figure 16 Representative data for shank net segmental power (blue) and rate of energy change (red) during stance at walking speed 0.8 BH/s.

### 3.2.2 Shank Segmental Power at Push-off

The ankle plantar flexors are known to generate high ankle power during push-off in late stance (Neptune et al., 2001). The flow of this power through the shank segment is of particular interest with respect to the design of biomimetic prosthetic devices. Figure 17 depicts a visual representation of the power balance of the shank at 90% of stance (peak ankle power) for one representative participant walking at 0.8 BH/s. Positive terms indicate power delivered to the segment; negative values correspond to outflows of power from the segment. At the selected point in stance, 6.46 W/kg of power flowed into the shank and 1.99 W/kg flowed out via the distal and proximal joint force power terms ( $P_{shank\_dj}$  and  $P_{shank\_pj}$ ), respectively. This outflow of power was predominately in the anterior direction, as the vertical velocity of the knee joint center at this point in stance was negligible (Section 3.1.2). A summary of all the segmental power terms for each participant at peak ankle power is provided in Table 6.

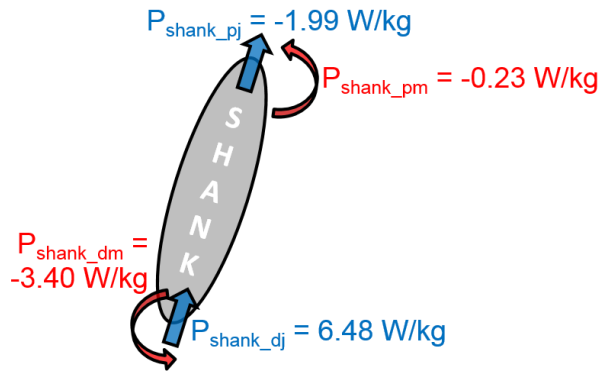


Figure 17 Visual representation of data for segmental power of the shank at peak ankle power (90% of stance) for one representative participant at walking speed 0.8 BH/s. The shank received 6.48 W/kg via the distal joint force power and released 1.99 W/kg via the proximal joint force power.

Table 6 Mean segmental power terms for all participants at peak ankle power

Participant	Distal Joint Force Power	Distal Muscle Moment Power	Proximal Joint Force Power	Proximal Muscle Moment Power
1	5.65	-3.47	-1.01	-0.10
2	6.50	-4.13	-0.87	0.02
3	5.93	-3.61	-1.15	-0.17
4	7.61	-4.41	-1.47	-0.09
5	5.11	-3.38	-1.11	0.07
6	5.83	-3.38	-1.31	-0.33
7	5.00	-2.71	-1.17	-0.13
8	6.02	-3.89	-0.87	-0.47
9	5.24	-3.45	-0.78	-0.64
10	6.48	-3.40	-1.99	-0.23
Mean ± SD:	5.94 ± 0.78	-3.58 ± 0.47	-1.17 ± 0.36	-0.21 ± 0.22

### 3.3 Telescoping Inverted Pendulum Shank Model

The feasibility of replicating the kinematics and energetics of shank progression via a non-biomimetic, telescoping inverted pendulum (TIP) shank model

was explored. As per Section 2.3.4.2 of the Approach, the position of the model ankle was fixed at a pivot point located at the position of the natural ankle joint center at the end of the ankle rocker of stance. Then, as per Section 2.3.6, with their angular orientation preserved, the shank segments during the forefoot and toe rockers were collapsed to emanate from this point and made to elongate based on an exponential function in order to mimic the natural knee joint center trajectory (Figure 18).

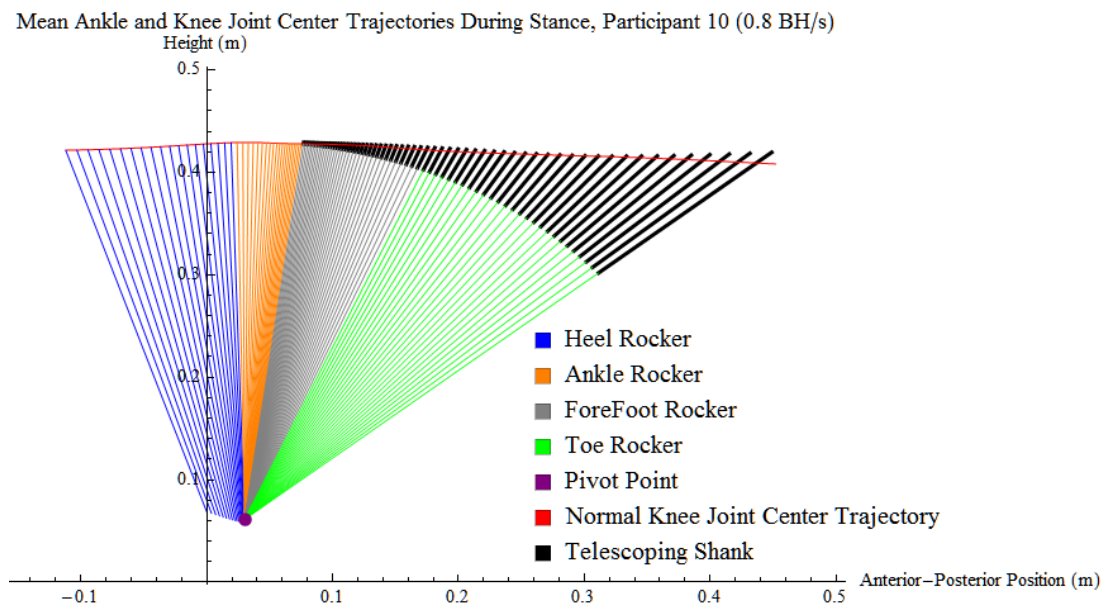


Figure 18 The telescoping shank was computed by collapsing all forefoot and toe rocker ankle positions to a pivot point (purple); fitting an exponential function to the distance between the collapsed knee joint center trajectory (gray and green lines) and the natural knee joint center trajectory (red trace); and elongating the shank based on the calculated exponential function to mimic the natural knee joint center trajectory.

The rate of expansion of the telescoping mechanism was calculated by curve fitting the distance between the collapsed and natural knee joint center trajectories.

The best fit to the data proved to be an exponential function:

$$\text{Telescoping Distance} = Ae^{k(t-1)} \quad (3.11)$$

Figure 19 shows the distance between the collapsed knee joint center trajectory and the natural knee joint center versus percent stance of the forefoot and toe rockers, along with the exponential fit to the data.

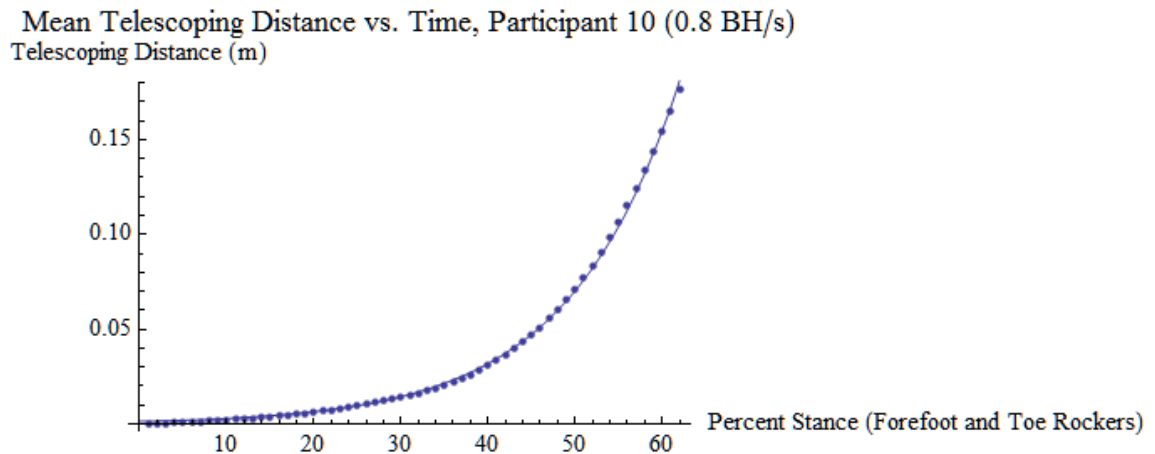


Figure 19 Representative plot of telescoping distance and exponential fit during the forefoot and toe rockers of stance at walking speed 0.8 BH/s. For this participant, telescoping distance was equal to  $0.0015e^{0.079(t-1)}$ .

The average maximum distance the telescoping shank elongated at the end of stance was  $0.164 \pm 0.026$  meters. The maximum telescoping distances for each participant are provided in Table 7.

Table 7 Maximum telescoping distance

<b>Participant</b>	<b>Maximum Telescoping Distance (m)</b>
1	0.169
2	0.181
3	0.123
4	0.203
5	0.148
6	0.149
7	0.184
8	0.176
9	0.126
10	0.176
Mean $\pm$ SD:	0.164 $\pm$ 0.026

### 3.3.1 Telescoping Knee Joint Center Position

To evaluate the use of the TIP shank model from a kinematic standpoint, the knee joint center trajectory resulting from the telescoping model was compared to the observed natural knee joint center positions. Across all 10 participants and the three gait events during which the shank was elongated (heel off, maximum dorsiflexion, toe off), the mean [limits of agreement] of the difference between the telescoping knee horizontal position and the motion capture-derived knee position was 0.002 [-0.006, 0.010] meters with ICC (3,2) = 0.995. (See Appendix A for breakdown by gait event.) For the vertical knee positions, the mean [limits of agreement] of the difference was 0.002 [-0.013, 0.005] meters with ICC (3,2) = 0.971.

### 3.3.2 Telescoping Shank Powers

To assess the validity of the TIP shank model from an energetics perspective, calculations of telescoping shank power ( $P_{telescoping}$ ) were made at the distal and proximal ends of the telescoping shank and compared to the respective shank joint force powers (Section 2.3.6.1). Figure 20 depicts the distal shank telescoping power

and distal shank joint force power for one representative participant walking at 0.8 BH/s. Across all 10 participants and the latter three gait events, the mean [limits of agreement] of the difference between the distal shank telescoping power and the distal shank joint force power was 0.217 [-0.498, 0.153] W/kg with ICC (3,2) = 0.943. (See Appendix A for breakdown by gait event.)

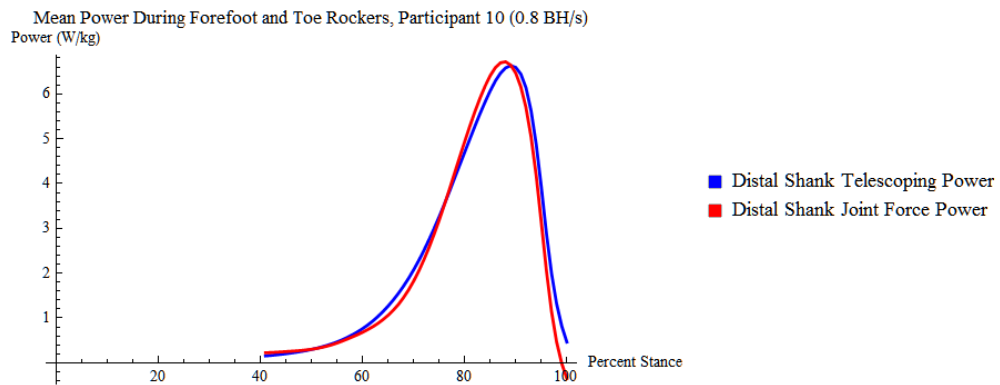


Figure 20 Distal shank telescoping power (blue) and distal shank joint force power (red) during stance for one representative participant at walking speed 0.8 BH/s.

Figure 21 depicts the proximal shank telescoping power and proximal shank joint force power for one representative participant walking at 0.8 BH/s. Across all 10 participants and the latter three gait events, the mean [limits of agreement] of the difference between the proximal shank telescoping power and the proximal shank joint force power was -0.152 [-0.577, 0.286] W/kg with ICC (3,2) = 0.848. (See Appendix A for breakdown by gait event.)

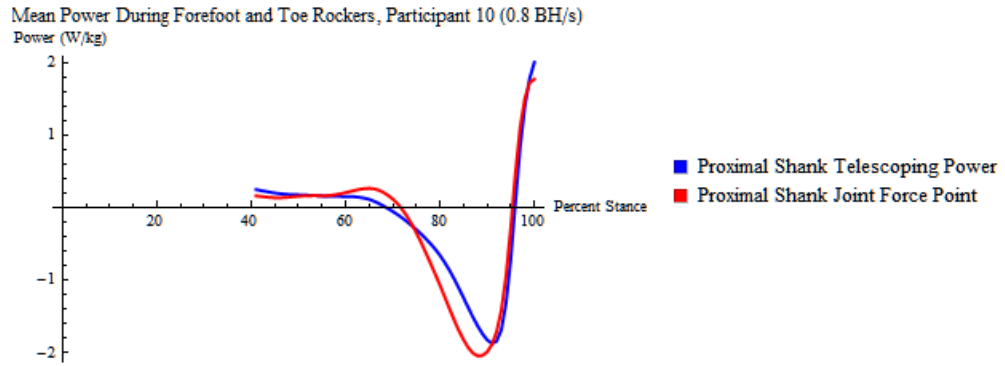


Figure 21 Proximal shank telescoping power (blue) and proximal shank joint force (red) power during stance for one representative participant at walking speed 0.8 BH/s.

## **Chapter 4**

### **DISCUSSION**

Individuals with transtibial amputation lack natural ankle-foot structures and thus rely on prostheses in order to ambulate. While prosthetic technology has improved dramatically since early designs, modern walking prostheses still fail to match human performance. The problem may be attributable to traditional analysis techniques and biomimetic design criteria. Efforts to mimic the human anatomy based on roll-over shape with unpowered devices and ankle power generation with bionic devices are well-intentioned but incomplete. In recent years, the progression of the shank during stance has actually been shown to be an important determining factor for many kinematic and kinetic aspects of gait (Owen, 2004). The overall purpose of the present study was to fully characterize the kinematics and energetics of shank progression during the stance phase of typical gait and to develop and evaluate alternate, non-biomimetic means of reproducing natural shank progression. As hypothesized, these analyses supported the innovation of a telescoping inverted pendulum (TIP) model of a prosthetic shank that would replicate shank rotation and translation as well as the energetics of push-off.

#### **4.1 Kinematics of Shank Progression**

In order to determine the relationships between foot and ankle rotation and shank kinematics during the stance phase of gait, a sagittal plane model was developed. This model was described in Section 2.3.4.1 of the Approach. Section 3.1

of the Results showed the model was valid, with strong correlations between model-based and motion capture-derived values ( $ICC(3,2) > .936$ ) on all measures, as hypothesized. Compared to a previous kinematic model (Ren et al., 2010), which utilized polar functions and polar angles to calculate sagittal plane ankle positions, the model presented herein was less mathematically complex and just as accurate. Like Ren et al.'s model, the largest differences between model and motion capture-values occurred at the gait events of heel strike and toe off, where the errors can be attributed to skin movement artefacts and soft tissue deformation.

Rotational shank kinematics were characterized by rotation in the direction of forward progress due predominantly to foot-to-floor motion in early and late stance and ankle motion in midstance. As measured by the trajectory of its proximal endpoint, the shank translated in the anterior direction during the ankle and forefoot rockers due to foot-to-floor motion and ankle dorsiflexion. During the toe rocker, it continued to progress forward due to foot-to-floor rotation, but with ankle plantar flexion actually working to counteract forward progression. The combined action of foot and ankle motion served to maintain the knee joint center at a relatively constant vertical height, which may be an essential feature of gait. During the forefoot and toe rockers, the shank appeared to rotate about a virtual fixed ankle position to within a very small error of  $0.003 \pm 0.002$  meters.

To predict the effects of walking with a fixed ankle (a worst-case approximation for a prosthetic ankle-foot) for one representative participant, the ankle angle was fixed to a neutral position and the trajectory of the shank during stance was predicted using the kinematic model. Figure 22 illustrates this trajectory, wherein the

position of the knee joint center drops off by over 0.1 meters during the toe rocker (green lines) due to the inability to plantar flex the ankle.

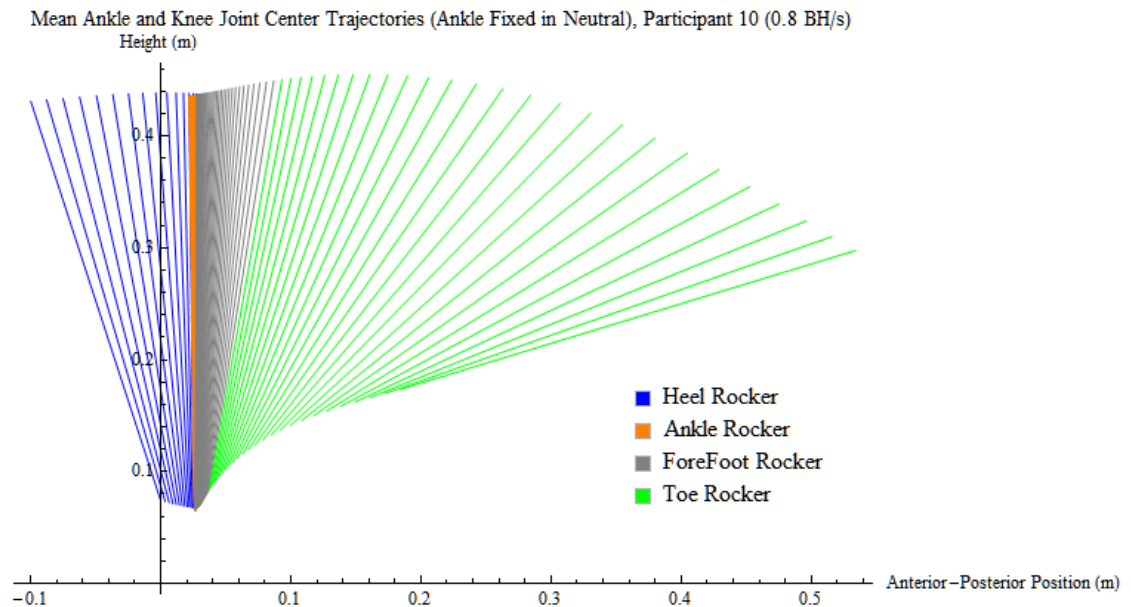


Figure 22 Model data for mean sagittal plane shank trajectory during stance at walking speed 0.8 BH/s with an ankle fixed in neutral alignment, colored by rocker. The height of the knee joint center drops off dramatically during the toe rocker (green lines).

Because energy-storing-and-returning prosthetic feet do, in fact, lack the ability to plantar flex far beyond neutral, when using these devices shank rotation is likely due primarily to foot-to-floor motion. To avoid excessive shank rotation approaching toe off, then, users must terminate the toe rocker early, which theoretically contributes to the asymmetrical stance times and step lengths exhibited in the laboratory (Isakov et al., 2000). Because reproducing plantar flexion in a biomimetic fashion is

disadvantageous in terms of mass distribution, the innovative, non-biomimetic TIP approach to replicating shank kinematics was warranted.

#### **4.2 Energetics of Shank Progression**

In Section 2.3.5 of the Approach, the method of quantifying push-off using the flow of mechanical power into and out of the distal and proximal shank was described. Section 3.2.1 of the Results showed that the shank gained energy over the course of stance. A slightly less than moderate correlation ( $ICC(3,2) = 0.739$ ) existed between the model-based and motion capture-derived data. These results are consistent with previous work, as are the errors, which resulted from the restriction of the analysis to the sagittal plane (Siegel et al., 1996; Robertson & Winter, 1980). Energetics analyses at the point in stance at which peak ankle power occurred revealed that power entered the shank distally via the joint force power and left proximally (also via the joint force power) in the anterior, not vertical, direction. These dynamics of energy flow suggest the possibility of replication via a TIP shank mechanism.

#### **4.3 Telescoping Inverted Pendulum Shank Model**

The goal of the TIP shank model was to determine the feasibility of inputting the natural quantities of energy into the system while preserving typical shank kinematics using a non-biomimetic approach. The ankle-foot was observed to behave equivalently to a telescoping (elongating) inverted pendulum, with the rotation of the shank occurring about a virtual fixed ankle position, or pivot point, located at the position of the ankle joint center at the end of the ankle rocker. The essential kinematic features to replicate with the elongation of the shank were the consistent

height and anterior translation of its proximal endpoint (defined by the knee joint center).

As described in Section 3.1.2 of the Results, correlations between the horizontal and vertical model-based and natural knee joint center positions were very high (ICC (3,2) > 0.971), as were correlations between proximal and distal powers (ICC (3,2) > 0.848), thereby confirming the hypotheses. The maximum distance the shank elongated was  $0.164 \pm 0.026$  meters. For perspective, this length was 0.014 meters longer than the average foot length of the participants. Remarkably, the rate at which the shank elongated in the TIP model followed an exponential function. This function would be a simple design criterion for a device.

Altogether, the results of this study strongly support the use of the TIP shank model for replicating the kinematics and energetics of typical gait, with one additional advantage over traditional designs being that the weight of the TIP shank would be concentrated more proximally, thereby improving user comfort and control.

#### **4.4 Delimitations and Future Directions**

Today's energy-storing-and-returning running-specific prostheses allow individuals with amputation to reach speeds approaching those of runners without missing limbs (Hobara, 2014). They do so, of course, in a non-biomimetic fashion, through material deformation and elastic recoil. The devices neither look nor function exactly like the human anatomy that they replace. Yet when it comes to walking, recent prosthetic design efforts have been focused on reproducing gait with bulky biomimetic ankle-feet. Injecting additional energy into the system is essential to improving function, but there may be a better method. More work must be done to analyze the shank progression of individuals wearing both energy-storing-and-

returning prosthetic ankle-feet and bionic ones at a variety of walking speeds in order to fully characterize these systems and their deficiencies.

Although the sample size of this study was relatively small, the data supported the notion that a non-biomimetic approach to prosthetic design may be well suited for reproducing the kinematics and energetics of the shank during push-off, at least in the sagittal plane and at the normal walking speed under consideration. In the future, the heel and ankle rockers of stance, as well as the swing phase of the gait cycle, will need to be characterized. The implications on the kinetics during swing for a rapidly contracting shank are as yet unknown. During the ankle and heel rockers of stance, a short, inexpensive SACH prosthetic foot based on roll-over shape may suffice. Once these additional investigations of stance and swing have been made, simulations can be performed to further validate the model. Finally, an actual TIP prosthetic shank could be designed, fabricated, and tested on individuals with transtibial, or perhaps even bilateral, amputation to determine if it could, indeed, help them achieve their highest level of function.

## REFERENCES

- Adamczyk, P., Collins, S. & Kuo, A., 2006. The advantages of a rolling foot in human walking. *Journal of Experimental Biology*, 209, pp.3953–3963.
- Anon, 2015. Tutorial: Foot and Ankle Angles. *Visual3D Wiki Documentation*.  
[http://www.c-motion.com/v3dwiki/index.php?title=Tutorial:\\_Foot\\_and\\_Ankle\\_Angles](http://www.c-motion.com/v3dwiki/index.php?title=Tutorial:_Foot_and_Ankle_Angles).
- Bland, J. & Altman, D., 1986. Statistical methods for assessing agreement between two methods of clinical measurement. *The lancet*, 327, pp.307–310.
- Blough, D.K. et al., 2010. Prosthetic cost projections for servicemembers with major limb loss from Vietnam and OIF/OEF. *The Journal of Rehabilitation Research and Development*, 47(4), p.387.
- Capute, A. et al., 1985. Normal gross motor development: The influences of race, sex and socioeconomic status. *Developmental Medicine & Child Neurology*, 27, pp.635–643.
- Cherelle, P. et al., 2014. Advances in propulsive bionic feet and their actuation principles. *Advances in Mechanical Engineering*, Article 98, pp.1–21.
- Curtze, C. et al., 2009. Comparative roll-over analysis of prosthetic feet. *Journal of Biomechanics*, 42, pp.1746–1753.
- Ferris, A.E. et al., 2012. Evaluation of a powered ankle-foot prosthetic system during walking. *Archives of physical medicine and rehabilitation*, 93(11), pp.1911–8.
- Fey, N.P., Klute, G.K. & Neptune, R.R., 2011. The influence of energy storage and return foot stiffness on walking mechanics and muscle activity in below-knee amputees. *Clinical Biomechanics*, 26(10), pp.1025–1032.
- Fridman, A., Ona, I. & Isakov, E., 2003. The influence of prosthetic foot alignment on trans-tibial amputee gait. *Prosthetics and orthotics international*, 27, pp.17–22.
- Gard, S. & Childress, D., 2001. What determines the vertical displacement of the body during normal walking? *JPO: Journal of Prosthetics and Orthotics*, 13(3), p.64.

- Geil, M.D. et al., 2000. Comparison of methods for the calculation of energy storage and return in a dynamic elastic response prosthesis. *Journal of Biomechanics*, 33, pp.1745–1750.
- Gutfleisch, O., 2003. Peg legs and bionic limbs: the development of lower extremity. *Interdisciplinary Science Reviews*, 28(2), pp.139–148.
- Hafner, B. et al., 2002a. Energy storage and return prostheses: does patient perception correlate with biomechanical analysis? *Clinical Biomechanics*, 17, pp.325–344.
- Hafner, B. et al., 2002b. Transtibial energy-storage-and-return prosthetic devices : A review of energy concepts and a proposed nomenclature. *Journal of Rehabilitation Research and Development*, 39(1), pp.1–11.
- Hansen, A.H., Childress, D.S., Miff, S.C., et al., 2004. The human ankle during walking: implications for design of biomimetic ankle prostheses. *Journal of biomechanics*, 37(10), pp.1467–1474.
- Hansen, A.H. & Childress, D.S., 2010. Investigations of roll-over shape: implications for design, alignment, and evaluation of ankle-foot prostheses and orthoses. *Disability and rehabilitation*, 32(26), pp.2201–9.
- Hansen, A.H., Childress, D.S. & Knox, E.H., 2000. Prosthetic foot roll- over shapes with implications for alignment of transtibial prostheses. *Prosthetics and Orthotics International*, 24(3), pp.205–215.
- Hansen, A.H., Childress, D.S. & Knox, E.H., 2004. Roll-over shapes of human locomotor systems: effects of walking speed. *Clinical biomechanics (Bristol, Avon)*, 19(4), pp.407–14.
- Hobara, H., 2014. Running-specific prostheses: The history, mechanics, and controversy (特集 アダプテッドスポーツの用具支援と技術支援). *Journal of the Society of Biomechanics*, 38(2), pp.1–6.
- Hof, A. et al., 1992. Calf muscle work and segment energy changes in human treadmill walking. *Journal of electromyography and kinesiology*, 2(4), pp.203–216.
- Holden, J.P. & Stanhope, S.J., 1998. The effect of variation in knee center location estimates on net knee joint moments. *Gait and Posture*, 7, pp.1–6.

- Isakov, E., Keren, O. & Benjuya, N., 2000. Trans-tibial amputee gait: Time-distance parameters and EMG activity. *Prosthetics and Orthotics International*, 24, pp.216–220.
- Kepple, T.M., Lohmann, K. & Stanhope, S.J., 1997. Relative contributions of the lower extremity joint moments to forward progression and support during gait. *Gait & Posture*, 6, pp.1–8.
- Knox, E., 1996. The role of prosthetic feet in walking. *PhD Thesis, Northwestern University, Evanston, Illinois, USA*.
- Van der Linde, H., Hofstad, C.J. & Geurts, A.C.H., 2004. A systematic literature review of the effect of different prosthetic components on human functioning with a lower limb prosthesis. *Journal of Rehabilitation Research and Development*, 41(4), pp.555–570.
- McGeer, T., 1990. Passive Dynamic Walking. *International Journal of Robotics Research*, 9(2), pp.62–82.
- Meier, M., Sam, M. & Hansen, A., 2004. The 'Shape & Roll' Prosthetic Foot: Field Testing in El Salvador. *Medicine, Conflict, and Survival*, 20(4), pp.307–325.
- Neptune, R.R., Kautz, S.A. & Zajac, F.E., 2001. Contributions of the individual ankle plantar flexors to support, forward progression and swing initiation during walking. *Journal of Biomechanics*, 34, pp.1387–1398.
- Nielsen, D. et al., 1989. Comparison of energy cost and gait efficiency during ambulation in below-knee amputees using different prosthetic feet-A preliminary report. *Journal of Prosthetics and Orthotics*, 1(1), pp.24–31.
- NLLIC, 2007. Fact Sheet: Limb Loss in the United States. *National Limb Loss Information Center*. [http://www.amputee-coalition.org/fact\\_sheets/limbloss\\_us.html](http://www.amputee-coalition.org/fact_sheets/limbloss_us.html).
- Owen, E., 2004. Shank angle to floor measures and tuning of “ankle-foot orthosis footwear combinations” for children with cerebral palsy, spina bifida and other conditions. *Master's Thesis, University of Strathclyde, Glasgow, United Kingdom*.
- Perry, J., Burnfield, J.M., & Cabico, L.M., 2010. *Gait Analysis: Normal and Pathological Function*. Thorofare, NJ: SLACK.

- Ren, Lei et al., 2010. A generic analytical foot rollover model for predicting translational ankle kinematics in gait simulation studies. *Journal of biomechanics*, 43(2), pp.194–202.
- Robertson, D. & Winter, D., 1980. Mechanical energy generation, absorption and transfer amongst segments during walking. *Journal of Biomechanics*, 13, pp.845–854.
- Rosenrot, P., Wall, J. & Charteris, J., 1980. The relationship between velocity, stride time, support time and swing time during normal walking. *Journal of Human Movement Studies*, 6, pp.323–335.
- Sanderson, D. & Martin, P., 1997. Lower extremity kinematic and kinetic adaptations in unilateral below-knee amputees during walking. *Gait & posture*, 6, pp.126–136.
- Siegel, K.L., Kepple, T.M. & Caldwell, G.E., 1996. Technical Note: Improved agreement of foot segmental power and rate of energy change during gait: inclusion of distal power terms and use of three-dimensional models. *Journal of Biomechanics*, 29(6), pp.823–827.
- Silverman, A.K. et al., 2008. Compensatory mechanisms in below-knee amputee gait in response to increasing steady-state walking speeds. *Gait & Posture*, 28(4), pp.602–609.
- Srinivasan, S., Raptis, I. a & Westervelt, E.R., 2008. Low-dimensional sagittal plane model of normal human walking. *Journal of biomechanical engineering*, 130(5), pp.1–11.
- Stein, J. & Flowers, W., 1987. Stance phase control of above-knee prostheses: knee control versus SACH foot design. *Journal of biomechanics*, 20(1), pp.19–28.
- Versluys, R. et al., 2009. Prosthetic feet: state-of-the-art review and the importance of mimicking human ankle-foot biomechanics. *Disability and Rehabilitation: Assistive Technology*, 4(2), pp.65–75.
- Weir, J., 2005. Quantifying test-retest reliability using the intraclass correlation coefficient and the SEM. *The Journal of Strength & Conditioning Research*, 19(1), pp.231–240.
- Winter, D., 2009. *Biomechanics and Motor Control of Human Movement* 4th ed., Hoboken, NJ: John Wiley & Sons, Inc.

Winter, D., 1983. Energy generation and absorption at the ankle and knee during fast, natural, and slow cadences. *Clinical Orthopaedics and Related Research*, (175), pp.147–154.

Winter, D. & Sienko, S., 1988. Biomechanics of below-knee amputee gait. *Journal of biomechanics*, 21(5), pp.361–367.

Ziegler-Graham, K. et al., 2008. Estimating the prevalence of limb loss in the United States: 2005 to 2050. *Archives of physical medicine and rehabilitation*, 89(3), pp.422–9.

**Appendix A**  
**SUPPLEMENTAL DATA**

Table 8 Ankle angle excursions, by rocker

<b>Participant</b>	<b>Heel Rocker (°)</b>	<b>Ankle Rocker (°)</b>	<b>Forefoot Rocker (°)</b>	<b>Toe Rocker (°)</b>	<b>Total (°)</b>
1	1.30	10.99	1.30	-33.97	-20.38
2	1.58	7.70	3.71	-32.75	-19.76
3	4.03	16.02	3.98	-27.66	-3.63
4	0.28	13.06	6.28	-40.87	-21.25
5	1.41	14.21	3.84	-31.04	-11.58
6	4.10	11.47	4.47	-31.21	-11.17
7	2.37	7.43	-0.42	-35.52	-26.14
8	2.24	11.02	4.94	-34.74	-16.54
9	0.06	10.00	5.08	-25.11	-9.97
10	0.14	8.44	8.32	-36.37	-19.47
Mean ± SD:	1.75 ± 1.39	11.03 ± 2.67	4.15 ± 2.30	-32.92 ± 4.26	-15.99 ± 6.39

Table 9 Foot-to-floor angle excursions, by rocker

<b>Participant</b>	<b>Heel Rocker (°)</b>	<b>Ankle Rocker (°)</b>	<b>Forefoot Rocker (°)</b>	<b>Toe Rocker (°)</b>	<b>Total (°)</b>
1	-19.06	-0.85	-2.96	-63.40	-86.27
2	-20.41	-0.19	-7.74	-57.06	-85.40
3	-10.10	-0.33	-5.72	-46.12	-62.26
4	-19.49	-0.14	-4.90	-64.34	-88.87
5	-16.76	0.64	-6.34	-56.69	-79.15

6	-13.69	-0.37	-4.80	-59.03	-77.90
7	-12.38	0.12	-5.81	-69.45	-87.52
8	-16.82	0.24	-4.16	-65.45	-86.19
9	-15.45	0.38	-6.62	-49.98	-71.68
10	-16.14	0.12	-7.56	-62.73	-86.31
Mean $\pm$ SD:	-16.03 $\pm$ 3.09	-0.04 $\pm$ 0.41	-5.66 $\pm$ 1.42	-59.42 $\pm$ 6.84	-81.16 $\pm$ 8.11

Table 10 Shank angle excursions, by rocker

Participant	Heel Rocker (°)	Ankle Rocker (°)	Forefoot Rocker (°)	Toe Rocker (°)	Total (°)
1	-20.02	-0.85	-3.99	-30.41	-55.27
2	-20.19	-0.19	-11.87	-29.95	-62.19
3	-9.43	-0.33	-10.77	-23.34	-43.86
4	-19.03	-0.14	-11.20	-27.97	-58.33
5	-17.11	0.64	-10.08	-27.36	-53.90
6	-17.45	-0.37	-9.02	-28.16	-55.00
7	-15.29	0.12	-5.21	-34.94	-55.31
8	-18.88	0.24	-9.06	-32.28	-59.98
9	-15.93	0.38	-11.33	-25.28	-52.16
10	-16.68	0.12	-15.34	-26.85	-58.75
Mean $\pm$ SD:	-17.00 $\pm$ 2.98	-0.04 $\pm$ 0.41	-9.79 $\pm$ 3.10	-28.65 $\pm$ 3.20	-55.48 $\pm$ 4.83

Table 11 Bland-Altman mean differences averaged across participants, by gait event

Outcome Variable (units)	Heel Strike	Foot Flat	Heel Off	Max. DF	Toe Off	Absolute Mean
Shank Angle (degrees)	-0.940	-0.164	-0.041	0.005	-2.125	0.655
Y Knee (m)	0.003	0.002	0.002	0.002	-0.003	0.002

Z Knee (m)	-0.004	-0.007	-0.001	-0.003	-0.014	0.006
Shank Segmental Power (W/kg)	-0.098	-0.097	-0.112	-0.051	-0.010	-0.073
Y Knee, Telescoping (m)			0.007	-0.001	0.000	0.002
Z Knee, Telescoping (m)			-0.003	-0.003	-0.005	0.002
Distal Shank Telescoping Power (W/kg)			0.189	0.095	-0.803	0.217
Proximal Shank Telescoping Power (W/kg)			-0.030	-0.197	-0.230	-0.152

Table 12 Bland-Altman mean lower limits of agreement averaged across participants, by gait event

<b>Outcome Variable (units)</b>	<b>Heel Strike</b>	<b>Foot Flat</b>	<b>Heel Off</b>	<b>Max. DF</b>	<b>Toe Off</b>	<b>Mean</b>
Shank Angle (degrees)	-3.808	-0.617	-0.670	-0.687	-6.590	-2.474
Y Knee (m)	-0.019	-0.004	-0.005	-0.004	-0.028	-0.012
Z Knee (m)	-0.012	-0.012	-0.008	-0.008	-0.040	-0.016
Shank Segmental Power (W/kg)	-0.098	-0.097	-0.112	-0.051	-0.010	-0.073
Y Knee, Telescoping (m)			-0.006	-0.005	-0.026	-0.013
Z Knee, Telescoping (m)			-0.407	-0.084	-1.003	-0.498
Distal Shank Telescoping Power (W/kg)			-0.006	-0.005	-0.026	-0.013
Proximal Shank Telescoping Power (W/kg)			-0.301	-0.736	-0.694	-0.577

Table 13 Bland-Altman mean upper limits of agreement averaged across participants, by gait event

<b>Outcome Variable (units)</b>	<b>Heel Strike</b>	<b>Foot Flat</b>	<b>Heel Off</b>	<b>Max. DF</b>	<b>Toe Off</b>	<b>Mean</b>
Shank Angle (degrees)	1.928	0.290	0.588	0.697	2.340	1.169

Y Knee (m)	0.025	0.007	0.010	0.007	0.022	0.014
Z Knee (m)	0.003	-0.002	0.006	0.002	0.012	0.004
Shank Segmental Power (W/kg)	0.003	0.057	0.253	0.043	0.077	0.087
Y Knee, Telescoping (m)			0.011	0.000	0.020	0.010
Z Knee, Telescoping (m)			0.001	-0.001	0.016	0.005
Distal Shank Telescoping Power (W/kg)			0.786	0.274	-0.602	0.153
Proximal Shank Telescoping Power (W/kg)			0.241	0.341	0.275	0.286

Table 14 Intraclass correlation (3,2), by gait event

<b>Outcome Variable</b>	<b>Heel Strike</b>	<b>Foot Flat</b>	<b>Heel Off</b>	<b>Max. DF</b>	<b>Toe Off</b>	<b>Mean</b>
Shank Angle	0.888	0.999	0.997	0.998	0.915	0.959
Y Knee	0.880	0.998	0.998	0.995	0.980	0.970
Z Knee	0.991	0.996	0.996	0.994	0.934	0.982
Shank Segmental Power	-0.098	-0.097	-0.112	-0.051	-0.010	-0.073
Y Knee, Telescoping			1.000	0.999	0.987	0.995
Z Knee, Telescoping			0.999	0.998	0.916	0.971
Distal Shank Telescoping Power			0.919	0.957	0.953	0.943
Proximal Shank Telescoping Power			0.900	0.797	0.846	0.848

Figure 23 Bland-Altman plots at heel strike. Data points are plotted with participant numbers. Solid lines represent the mean difference between measured and modeled values. Dashed lines represent the limits of agreement (mean  $\pm$  1.96 standard deviations).

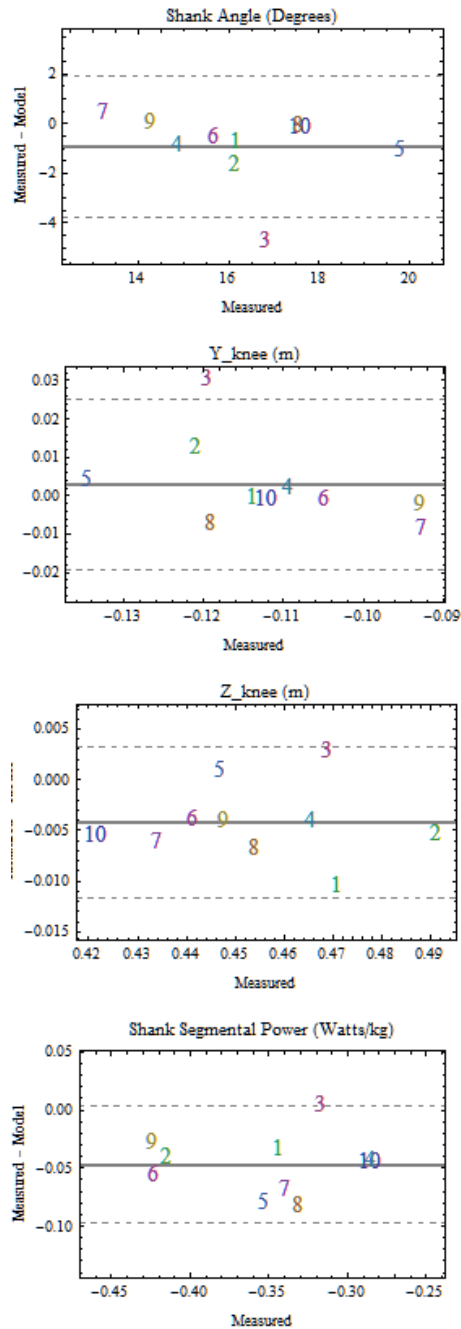


Figure 24 Bland-Altman plots at foot flat. Data points are plotted with participant numbers. Solid lines represent the mean difference between measured and modeled values. Dashed lines represent the limits of agreement (mean  $\pm$  1.96 standard deviations).

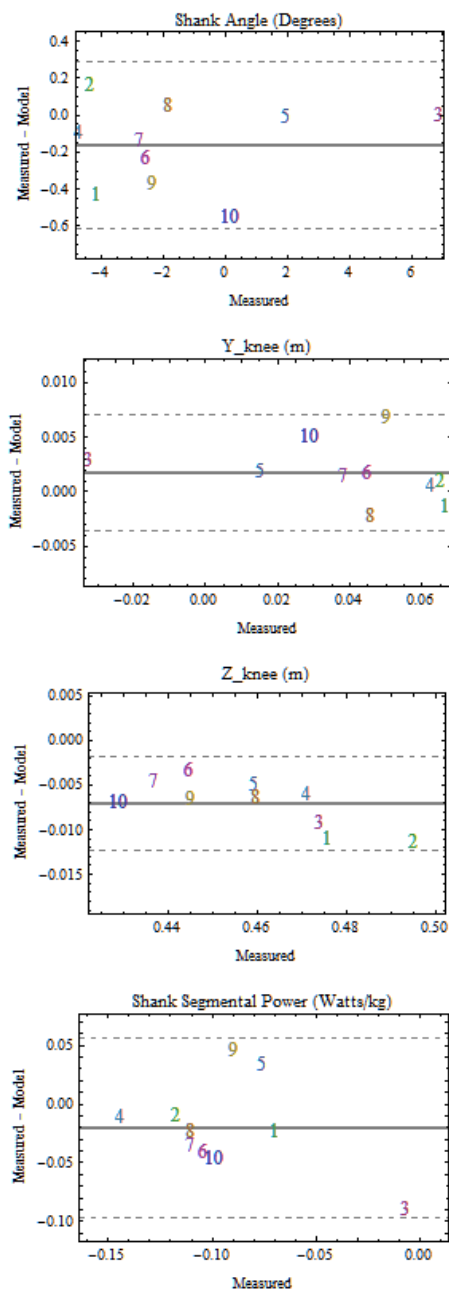


Figure 25 Bland-Altman plots at heel off. Data points are plotted with participant numbers. Solid lines represent the mean difference between measured and modeled values. Dashed lines represent the limits of agreement (mean  $\pm$  1.96 standard deviations).

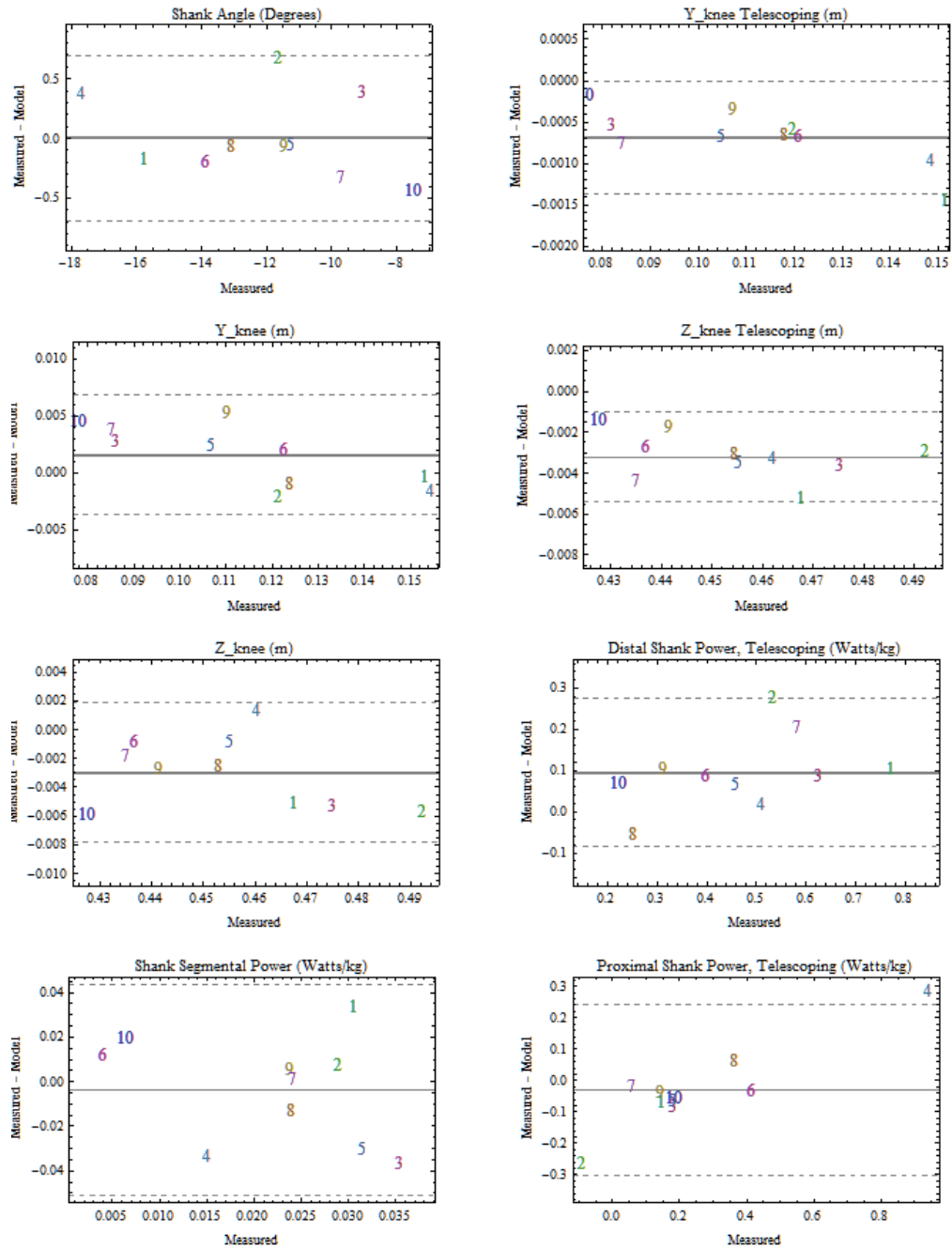


Figure 26 Bland-Altman plots at maximum dorsiflexion. Data points are plotted with participant numbers. Solid lines represent the mean difference between measured and modeled values. Dashed lines represent the limits of agreement (mean  $\pm$  1.96 standard deviations).

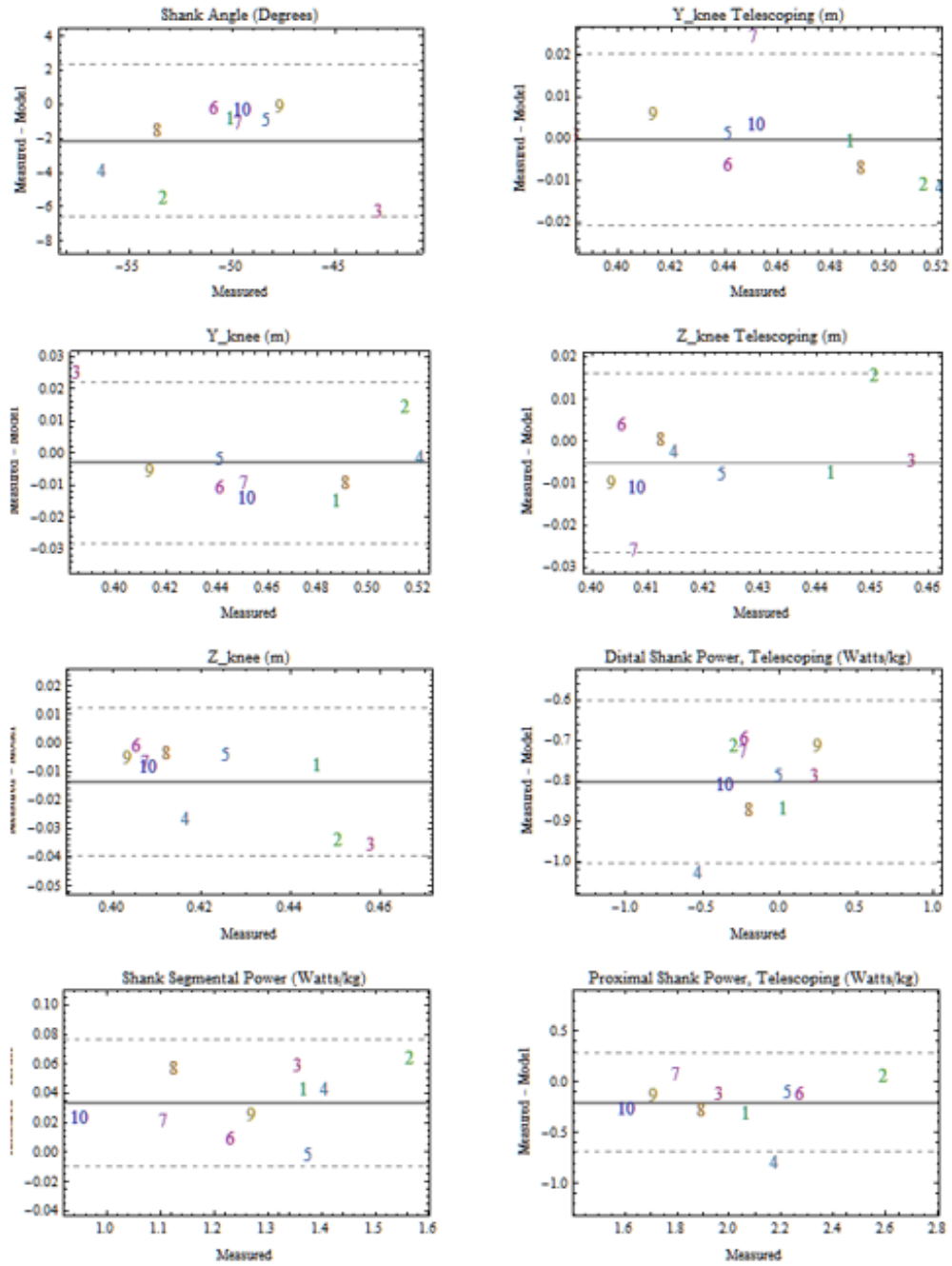
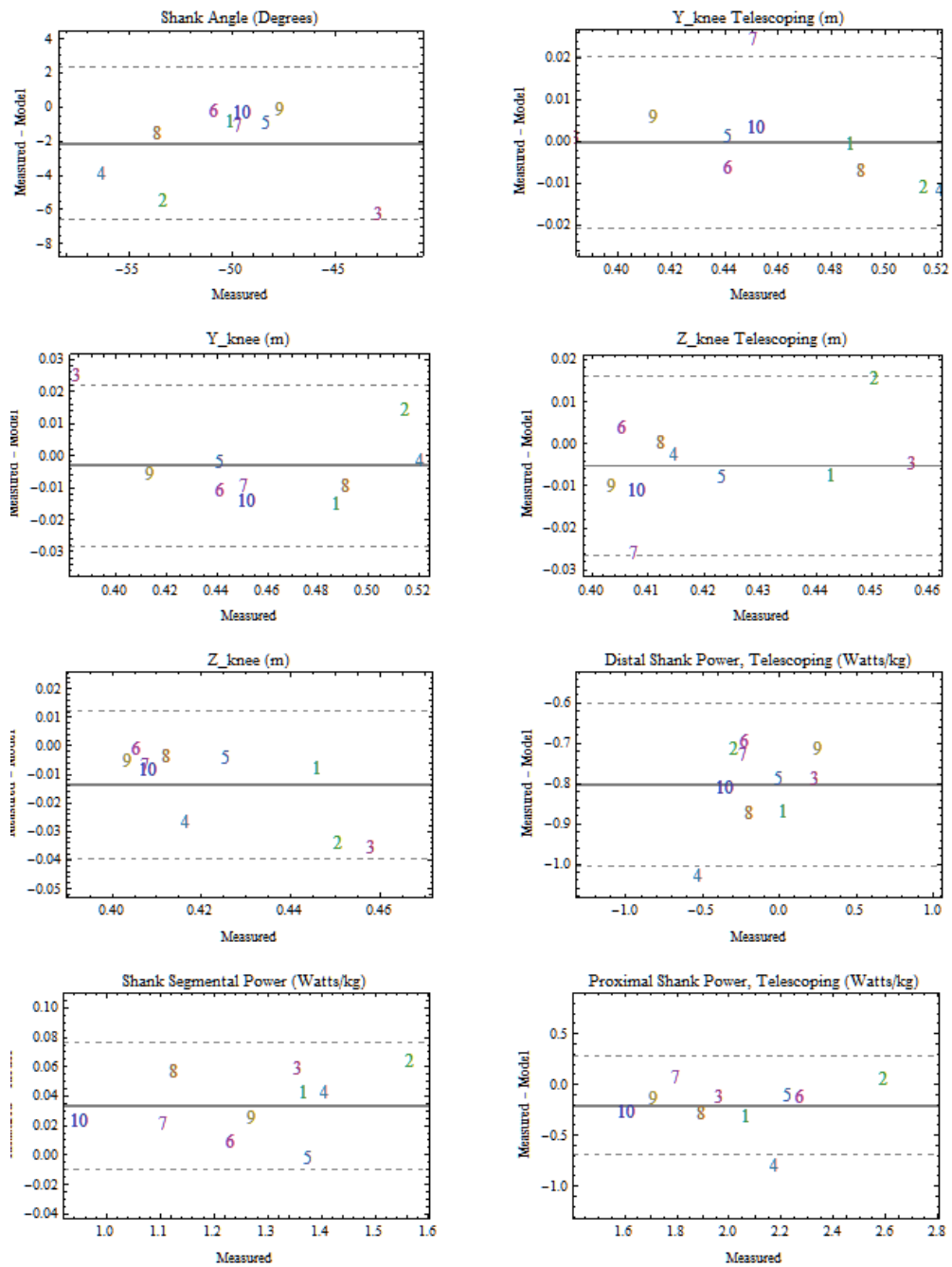


Figure 27 Bland-Altman plots at toe off. Data points are plotted with participant numbers. Solid lines represent the mean difference between measured and modeled values. Dashed lines represent the limits of agreement (mean  $\pm$  1.96 standard deviations).



## Appendix B

### INFORMED CONSENT

---

	<p><b>CONSENT TO PARTICIPATE IN A HUMAN SUBJECT RESEARCH STUDY</b></p> <ul style="list-style-type: none"><li>• Adult Subject</li></ul>
---	--

---

COLLEGE: **College of Health Sciences**

STUDY NUMBER: 324555-1

PRINCIPAL INVESTIGATOR: **Stanhope, Steven J.**

STUDY TITLE: **Human Movement Analysis Database**  
(HuMAD Protocol)

Latest IRB Review: 3/12/2015

Latest Amendment Approved: 9/02/2014

---

### INTRODUCTION

We invite you to take part in a research study at the University of Delaware (UD).

First, we want you to know that:

Taking part in research at the University of Delaware is entirely voluntary.

You may choose not to take part, or you may withdraw from the study at any time. In either case, you will not lose any benefits to which you are otherwise entitled.

You may receive no benefit from taking part. The research may give us knowledge that may help people in the future.

Now we will describe this research study. Before you decide to take part, please take as much time as you need to ask any questions and discuss this study with anyone at the University of Delaware, or with family, friends or your personal physician or other health professional.

#### PURPOSE OF THE STUDY

The purpose of this study is to collect information on the different ways people use rehabilitation devices, such as artificial legs or ankle braces to move when they walk, jog, or run. Scientists and doctors often compare information obtained from diverse groups of people to patient information in order to better understand the effects of disease and treatment on patient problems. You are being asked to participate in this study because we expect that you use normal patterns to move and we wish to see how your pattern of moving changes when you wear different types of artificial legs or braces.

#### PROCEDURE:

Before participating in this study, all of the movement tasks you will be asked to carry out will be explained by Dr. Stanhope or another member of the research team. The type of movement task (walk, jog, or run) you will be asked to perform will be determined in advance by the research team based on your prosthetic/orthotic prescription. You may wish to not perform a specific task and not to take part in the study. If you wish to continue, you will be asked to visit the University of Delaware for one or potentially more visits. A visual walking test will be performed by a member of the research team to determine how your joints move, how strong you are, and your comfortable walking speed. These procedures should not cause any discomfort.

During your instrumented movement test, you will be requested to wear a t-shirt and shorts. You may be asked to walk, jog, or run overground and/or on a treadmill. When walking on the treadmill, a body weight support system may be used during data collection. The support system is designed to safely provide constant body weight support up to 100% body weight, for individuals up to 150kg. This system includes an overhead harness system that will be

used as subjects walk over a split-belt treadmill. It is designed to catch subjects in the event of a fall and the harness can be quickly removed. Subjects will be fitted with an overhead harness.

Small plastic reflective balls will be attached to your body. To do this, your arms and legs will be wrapped with a soft, rubber-like material. A piece of firm material called a shell may then be attached to the rubber sleeves with Velcro or a self-adherent bandage. The small round balls may also be attached to your skin using an adhesive. After the reflective balls have been attached, the harness will then be secured to the body weight support system. Additionally, we may also want to test your muscles using electromyography (EMG). To do this, we will attach small metal electrodes to the surface of your skin using an adhesive. EMG is a measurement tool that is used to assess muscle function. Lastly, we may also ask you to breathe through an oxygen valve during the movement task to obtain a measurement of your metabolic energy expenditure. You should not feel any discomfort with these tests.

Once the above items are in place, you will be asked to perform a task several times while scientific cameras record the positions of the reflective balls. The cameras do not take pictures of your face or body parts. Each instrumented movement test will require a maximum of 2 hours to complete. You may rest at any time. Following the instrumented movement test, we will ask you to complete a questionnaire evaluating the performance of any artificial leg or brace you may wear.

If you are wearing an artificial leg or an ankle brace, you may be asked to repeat the protocol multiple times (in the same visit or different visits) with different types or settings of artificial legs or braces. However, you may decline our request and ask to stop participating at any time. If the protocol is repeated within the same visit, you will be given ample time to get acclimated to moving with the different artificial leg or brace (a minimum of 5 minutes), until you feel stable, comfortable, and until you feel that your movement pattern is reproducible.

#### RISKS:

The risks involved in participating are minimal; no more than those incurred during normal walking, jogging, or running and customary training and supervised use of a rehabilitation device. There is a slight chance of a mild skin irritation from the attachment of adhesive circles to the skin during the gait analysis portion of the study. The soft, rubber-like material may feel

tight, but if it is uncomfortable or interferes with your movements, tell one of the investigators and it will be readjusted. This material may cause a skin irritation, but the material is worn only for a short period of time and skin reactions are rare. There is also a slight chance of skin irritation due to wearing an artificial leg or brace or the harness of the body weight support system; however, adjustments will be made so that you will remain as comfortable as possible. Your safety will be continuously monitored while you are walking, jogging, or running with the artificial legs or braces.

#### BENEFITS:

You are unlikely to receive any direct benefit from participating in this study.

#### COMPENSATION:

You will not receive compensation for participating in this study.

#### SUBJECT RIGHTS:

IF you have any questions or do not understand any part of this study, ask to speak with the Principal Investigator. This study is voluntary, and you may withdraw your consent to participate at any time.

You may be withdrawn from the study for one of the following reasons:

- failure to follow instructions
- the investigator decides that continuation could be harmful to you
- you need treatment not allowed in the study
- the study is canceled
- other administrative reason (e.g., necessary documentation is not in place at the time of the study)

#### **OTHER PERTINENT INFORMATION**

1. **Confidentiality.** When results of a University research study are reported in medical journals or at scientific meetings, the people who take part are not named and identified. In most cases, the University will not release any information about your research involvement without your written permission. However, if you sign a release of information form, for example, for an insurance company, the University will give the insurance company information from your instrumented movement analysis record. This



**CONSENT TO REVEAL SUBJECT IDENTITY  
(Not required for participation in this study)**

The data collected in this protocol may be useful to clinicians and healthcare providers to facilitate objective clinical decision-making on my behalf. Therefore, I hereby consent to allow my identity and associated data obtained in this protocol to be revealed to the following individual(s) or organization(s):

\_\_\_\_\_  
Name of individual/organization

\_\_\_\_\_  
Name of individual/organization

\_\_\_\_\_  
Name of individual/organization

\_\_\_\_\_  
Signature of Subject

\_\_\_\_\_  
Date

SUBJECT IDENTIFICATION  SUBJECT INITIALS:	<b>CONSENT TO PARTICIPATE IN A HUMAN SUBJECT RESEARCH STUDY</b> <ul style="list-style-type: none"><li>• Adult Subject</li></ul> File in Secure Records: Protocol Consent
---	--

## Appendix C

### HUMAN SUBJECTS PROTOCOL

University of Delaware

Protocol Title: Human Movement Analysis Database  
(HuMAD Protocol)

Principal Investigator

Name: Steven J. Stanhope, Ph.D.  
Department/Center: Kinesiology & Applied Physiology  
Contact Phone Number: 302-831-3496  
Email Address: Stanhope@udel.edu

Advisor (if student PI):

Name:  
Contact Phone Number:  
Email Address:

Other Investigators:

Investigator Assurance:

By submitting this protocol, I acknowledge that this project will be conducted in strict accordance with the procedures described. I will not make any modifications to this protocol without prior approval by the IRB. Should any unanticipated problems involving risk to subjects, including breaches of guaranteed confidentiality occur during this project, I will report such events to the Chair, Institutional Review Board immediately.

#### 1. Is this project externally funded?

If so, please list the funding source:

#### 2. Project Staff

Please list personnel, including students, who will be working with human subjects on this protocol (insert additional rows as needed):

<b>NAME</b>	<b>ROLE</b>	<b>HS TRAINING COMPLETE?</b>
Kota Takahasi, MBE	Student/Research Asst	Yes
Elisa Schrank, BS	Student/Research Asst	Yes
LaKisha Guinn, MBE	Student/Research Asst	Yes
Alexander Razzook, MSE	Student/Research Asst	Yes
John Horne, CPO	Certified Prosthetist/Orthotist	Yes

### 3. **Special Populations**

Does this project involve any of the following?

Research on Children? No

Research with Prisoners? No

Research with any other vulnerable population (please describe)? No

4. **RESEARCH ABSTRACT** Please provide a brief description in LAY language (understandable to an 8<sup>th</sup> grade student) of the aims of this project.

Rehabilitation devices like artificial legs and leg braces help people with lost or injured legs to stand, walk, run and play. Many advances have been made in the designs of artificial legs and braces. To customize the prescription of these devices, clinicians must often choose from a large list of settings, alignments and device characteristics. The prescription process is currently a form or art because the field of human movement analysis lacks methods for understanding how device characteristics and settings contribute to human movement tasks such as walking, running and jumping. Therefore, the primary purpose of the proposed project is to develop and use advanced methods of human movement analysis to relate normal, braced and artificial limb characteristics to the performance of movement tasks. After making sure it is safe for a person to participate, we will use a special motion capturing system in a laboratory setting to measure people as they perform movement tasks like walking, running or jumping. The resulting database will contain examples of how medically healthy people use normal, braced and artificial limbs to perform common movements. Our long term goal is to use the database to better understand how braces and artificial limbs help medically healthy people perform common movement tasks such as walking, running and jumping. We believe the techniques developed under and data contained within the human movement analysis database (HuMAD) will provide important information that one day will be used to better prescribe braces and artificial legs to assist patients with obtaining their highest ability to function.

5. **PROCEDURES** Describe all procedures involving human subjects for this protocol. Include copies of all surveys and research measures.

All testing will take place on the University of Delaware campus in a motion capture facility where each subject will undergo an instrumented movement analysis while they walk, jog, or run. For each subject with prescribed rehabilitation devices, the movement task he or she will perform will be determined based on their prosthetic/orthotic prescription. For example, if select individuals are prescribed running-specific prosthetic or orthotic devices, he or she will be asked to jog or run at their customary pace. In addition, normal subjects without any rehabilitation devices will be recruited to create a speed-matched database of walking, jogging, and running to facilitate direct comparisons of lower extremity mechanics. Prior to testing, the movement task the subjects will be performing will be determined, and we will obtain an informed consent from each subject. Data analyses related to lower extremity joint motions, net joint moments, and powers will be used to characterize overall behavior of persons moving with and/or without rehabilitation devices.

#### **Initial movement task test**

Prior to performing any movement task, subjects will undergo a guarded trial of the task during which they will be asked to repeatedly perform the movement task under the watch of a research assistant. In addition, subjects will be asked to provide a medical history regarding lower extremity injuries and conditions that might influence their walking ability. At this time, the type, characteristics, settings and configuration of any brace or artificial limb to be worn during the test session will be recorded.

#### **Instrumented Movement Analysis**

The following general data collection and analysis procedures constitute the technical aspects utilized in all instrumented movement analyses. Subject gait characteristics will be measured in the Human Performance Laboratory (HPL) or the Center for Mobility Enhancement (CeME) currently under development at 5 Innovation Way on the University of Delaware's campus, using a 6-camera motion capture system with ground force measurement capabilities. Subjects may be asked to walk, jog, or run overground at the HPL, and/or on an instrumented treadmill at the CeME.

Subjects will be asked to wear shorts and a t-shirt during testing. Clusters of 3 to 4 reflective spherical targets, 14mm in diameter, will be affixed to the body and extremities with neoprene or self-adhesive wraps. Additional targets will be placed with adhesive circles on the skin over bony landmarks used to designate segment ends and joint centers (Holden and Stanhope, 1998). Surface electromyographic (EMG) electrodes may be placed bilaterally near the motor points of primary lower extremity muscle groups. In addition, subjects may be asked to breathe through a valve to obtain estimates of oxygen consumption and metabolic energy expenditure during the movement tasks.

Anthropometric measurements will be made of each subject including height and body weight. An anthropometer will be used to measure select segment characteristics (e.g., forefoot width, ankle joint width, knee joint width, intertrochanteric distance, and pelvic width and depth). Analytic techniques will be developed in cases where artificial limbs or braces restrict access to or do not have like anatomic sites.

After the targets are affixed and anthropometric measures are made, a static subject calibration trial will be collected. The subject will stand upright in the middle of the motion capture image volume facing in the direction of walking in the laboratory with their feet pointed forward. The motion capture system will acquire the 3D locations of the reflective targets for a one second trial. Following this trial, gait trials will be collected.

For the overground walking trials, the subject will be asked to stand at the end of a 6 m walkway and walk across the laboratory floor. The motion capture system will acquire the 3D locations of the reflective targets on the body within the middle of 2 m of the walkway. Four force platforms, mounted in series flush with the floor within the 2 meter volume, will be used to sample the ground reaction forces from the three subsequent stance phases, with the stance phase of interest occurring centrally in the sequence. Subject starting position will be adjusted so that each foot makes an isolated contact on each force platform during each walking trial. An optically-based gait velocity indicator will provide walking velocity feedback. Using the gait velocity data as verbal feedback, subjects will be asked to walk at a percent of natural walking velocity until a minimum of three and a maximum of 10 trials are acquired. Subjects will be allowed to rest between walking trials upon request.

For walking trials on a treadmill, the belt speed will be controlled as a percent of the natural walking velocity. Force platforms mounted side-by-side beneath the belt will continuously capture the ground reaction force on each limb, while the motion capture system acquires the 3D locations of the reflective targets on the body. Subjects will be given ample time to get acclimated to walking on the treadmill. An overhead harness system will be used to ensure safety for each subject.

For jogging or running trials (overground or on a treadmill), the protocol will follow closely with the previously described walking trials. For subjects with prescribed running-specific prosthetic or orthotic devices, they will jog or run at their customary speed. For individuals without prosthetic/orthotic devices, the speeds will be targeted to match those of the subjects jogging or running with rehabilitation devices.

For participants wearing rehabilitation devices, they may be asked to repeat the protocol (overground or treadmill) multiple times wearing different types of devices they have been prescribed (in the same visit or different visits). The selection and adjustment of devices will be under the direction of a certified prosthetist/orthotist. For example, an individual with below-knee amputation may be asked to undergo the protocol wearing different types of or settings on artificial legs. An individual wearing a brace may repeat the protocol with different braces. If multiple devices are tested within the same visit, subjects will be given ample time (a minimum of 5 minutes) to get acclimated with the new device. Testing with the new device will proceed whenever the subjects subjectively indicate that his/her movement pattern feels stable, comfortable, and reproducible. Immediately following the instrumented gait analysis while using a particular rehabilitation device, the subjects will be asked to complete a questionnaire, adapted from the Prosthetic Evaluation Questionnaire (Legro et al, 1998), to subjectively evaluate the quality of a particular rehabilitation device.

## **6. STUDY POPULATION AND RECRUITMENT**

Describe who and how many subjects will be invited to participate. Include age, gender and other pertinent information. Attach all recruitment fliers, letters, or other recruitment materials to be used.

To develop the HuMAD, approximately 300 medically healthy subjects (males and females) who are over 18 years of age will be recruited via the word of mouth or by their clinician. For this project, the term healthy is defined as a lack of systemic disease that alters ability of subjects to participate in activities of their choice. In addition, healthy means no current pathology where there is any possibility of damage to muscle, ligament, or cartilage in the lower extremity.

In addition, the following people will be recruited:

- Individuals with lower extremity amputation and have prescribed artificial limbs.
- Individuals with impaired lower extremity function that have been prescribed a form of rehabilitation brace.

Describe what exclusionary criteria, if any will be applied.

Subjects with an unsafe, unsteady, or highly variable movement pattern upon visual observation will be excluded. Subjects who are unable to repeatedly execute the movement pattern in the desired manner will be excluded from participation

Describe what (if any) conditions will result in PI termination of subject participation.

A subject may be withdrawn from the study for any of the following reasons:

- failure to follow instructions
- the investigator decides that continuation could be harmful to the subject
- the study needs treatment not allowed in the study
- the study is canceled
- other administrative reason (e.g., necessary documentation is not in place at the time of the study)

## **7. RISKS AND BENEFITS**

Describe the risks to participants (risks listed here should be included in the consent document). If risk is more than minimal, please justify.

The risks involved in participating in the proposed series of non-invasive movement tasks are minimal. Much like any repeated gait test, there is a slight chance of suffering a fall and mild skin irritation from the attachment of adhesive circles to the skin during the movement task portion of the study.

What steps will be taken to minimize risks?

To minimize the risk of injury due to falls, subjects will be safely monitored by an investigator.

Describe any direct benefits to participants.

Subjects will receive no direct medical benefits from participation in this study. Compensation for time volunteered to this study will not be provided.

Describe any future benefits to this class of participants.

There are no future benefits to the participants.

If there is a Data Monitoring Committee (DMC) in place for this project, please describe when and how often it meets.

There is no Data Monitoring Committee for this project.

## **8. COMPENSATION**

Will participants be compensated for participation? No.

If so, please include details.

## **9. DATA**

Will subjects be anonymous to the researcher? No

If subjects are identifiable, will their identities be kept confidential? Yes

How and how long will data be stored?

The coded experimental data will be stored for a minimum of 10 years in a secure electronic database.

How will data be destroyed?

When the time comes, the data will be erased from the electronic database and the storage device formatted.

How will data be analyzed and reported?

The data obtained from the movement tasks (segment motions and ground reaction forces) will be input into Visual3D software (C-Motion Inc., Germantown, MD). Using Visual3D software, we will compute variables like joint motion (i.e., position, velocity, acceleration) and joint moments, and powers. In addition, we will use custom-analyses developed under this protocol and previously developed methods such as six degree-of-freedom ankle joint power (Buczek et al., 1994), distal foot power (Siegel et al., 1996), induced acceleration analysis (Kepple et al., 1997), power flow analysis (Siegel et al., 2004), natural ankle pseudo-stiffness (Razzook et al., 2011), roll-over dynamics

(Takahashi et al., 2011), and unified deformable segment power (Takahashi et al., 2011). These and new analyses will be used to compare lower extremity mechanics of persons wearing rehabilitation devices relative to the natural limb function database.

The results will be reported in a series of journal articles and presentations.

#### 10. **CONFIDENTIALITY**

Will participants be audiotaped, photographed or videotaped during this study?

Subjects may be photographed or videotaped. Any photographs and videotapes will be limited to a view from the shoulders to the feet so that the identification of the subject is protected.

How will subject identity be protected?

Each subject will be assigned a unique numerical subject identifier that will be used to label and track all data. Documents containing patient identifiers and the keys for breaking subject identification codes will be kept separately in a secured location with access limited to the PI.

Is there a Certificate of Confidentiality in place for this project? (If so, please provide a copy).

No

#### 11. **CONSENT and ASSENT**

Consent forms will be used and are attached for review.

Additionally, child assent forms will be used and are attached.

Consent forms will not be used (Justify request for waiver).

#### 12. **Other IRB Approval**

Has this protocol been submitted to any other IRBs? No

If so, please list along with protocol title, number, and expiration date.

#### 13. **Supporting Documentation**

Please list all additional documents uploaded to IRBNet in support of this application.

Adapted Prosthetic Evaluation Questionnaire – HuMAD Protocol.pdf  
Consent – HuMAD Protocol.pdf

Prosthetic-Orthotic Info Sheet – HuMAD Protocol.pdf  
Subject Contact Info form – HuMAD Protocol.pdf  
Subject screening form – HuMAD Protocol.pdf  
Anthro Measurements – HuMAD Protocol.pdf  
Trial Info Sheet – HuMAD Protocol.pdf  
Photo-Video consent – HuMAD Protocol.pdf

## References

Buczek FL, Kepple TM, Siegel KL, and Stanhope SJ. 1994. Translational and rotational joint power terms in a six degree-of-freedom model of the normal ankle complex. *Journal of Biomechanics*, 27, 1447-1457.

Holden, JP, and Stanhope SJ., 1998. The effect of variation in knee center location estimates on net knee joint moments. *Gait and Posture* 7, 1-6.

Kepple TM, Siegel KL, and Stanhope SJ., 1997. Relative contributions of the lower extremity joint moments to forward progression and support during stance. *Gait and Posture* 6, 1-8.

Legro MW, Reiber GD, Smith DG, del Aquila M, Larsen J, Boone D., 1998. Prosthetic Evaluation Questionnaire for persons with lower limb amputations: assessing prosthesis-related quality of life. *Archives of Physical Medicine and Rehabilitation* 79, 931-938.

Razzook AR, Takahashi KZ, Guinn LD, Schrank ES, and Stanhope SJ. Predictive model for natural ankle stiffness during walking: implications for ankle foot orthosis prescription. *Proceedings of the Gait and Clinical Movement Analysis Society Conference, Bethesda, Maryland, April 2011.*

Siegel KL, Kepple TM, and Caldwell GE, 1996. Improved agreement of foot segmental power and rate of energy change during gait: inclusion of distal power terms and the use of three-dimensional models. *Journal of Biomechanics* 29, 823-827.

Siegel KL, Kepple TM, and Stanhope SJ., 2004. Joint moment control of mechanical energy flow during normal gait. *Gait and Posture* 19, 69-75.

Takahashi KZ, Razzook AR, Guinn LD, Schrank ES, and Stanhope SJ. A model of normal gait roll-over dynamics: one step closer to customizing prosthetic ankle-foot components. *Proceedings of the Gait and Clinical Movement Analysis Society Conference, Bethesda, Maryland, April 2011.*

Takahashi KZ, Razzook AR, Guinn LD, Schrank ES, Kepple TM, and Stanhope SJ. A unified deformable segment model of the combined ankle-foot system that does work. *Proceedings of the annual meeting of the American Society of Biomechanics, Long Beach, CA, August 2011.*